DOKUZ EYLÜL UNIVERSITY
GRADUATE SCHOOL OF NATURAL AND APPLIED SCIENCES

SEA WATER EFFECT ON COMPOSITE PIPES SUBJECTED TO IMPACT LOADING

by
Murat SARI

June, 2010
İZMİR

SEA WATER EFFECT ON COMPOSITE PIPES SUBJECTED TO IMPACT LOADING

A Thesis Submitted to the
Graduate School of Natural and Applied Sciences of Dokuz Eylül University
In Partial Fulfillment of the Requirements for the Degree of Master of Science
in Mechanical Engineering, Mechanics Program

by

Murat SARI

June, 2010
İZMİR

M.Sc THESIS EXAMINATION RESULT FORM

We have read the thesis entitled **"SEA WATER EFFECT ON COMPOSITE PIPES SUBJECTED TO IMPACT LOADING"** completed by **MURAT SARI** under supervision of **PROF. DR. RAMAZAN KARAKUZU** and we certify that in our opinion it is fully adequate, in scope and in quality, as a thesis for the degree for Master of Science.

Prof. Dr. Ramazan KARAKUZU

Supervisor

(Jury Member)

(Jury Member)

Prof.Dr. Mustafa SABUNCU

Director

Graduate School of Natural and Applied Sciences

ACKNOWLEDGMENTS

First of all, I must express my sincere gratitude to my supervisor, Prof. Dr. Ramazan KARAKUZU, for his psychological and mental support and guidance throughout of the greatest contribution to the compilation of this study.

I also would like to express my gratitude to Prof. Dr. Onur SAYMAN, for his technical consequential support throughout all of the study.

I would like to thank research assistants M. Emin DENİZ, Aytaç GÖREN, mechanical engineer Tolga DOĞAN and technician Salih EKŞİ for their help during experimental stages of the study.

I would like to thank TÜBİTAK (The Scientific and Technological Research Council of Turkey) for supporting this study under Project number 108M471.

I would like to thank thanks "İzoreel", "Artipol" and "HPA" firms for their materials and instrument supports.

I wish to express my thanks to my brother students, Olgay DAĞDELEN and Yalın AKGÜN for their direct and indirect various friendly aids.

Finally, I would like to thank my parents for their continuous loving support throughout my all life and also I would like to my fiance for her inexhaustible passion, patience and understanding.

Murat SARI

SEA WATER EFFECT ON COMPOSITE PIPES SUBJECTED TO IMPACT LOADING

ABSTRACT

The aim of this experimental study was to investigate the sea water effect on fatigue behavior of composite pipes subjected to impact loads.

In this study, firstly, the general data about burst strength (load capacity) and average life cycle of fatigue composite pipes are given. Manufacturing of vessels by filament winding method is expressed. Schematic of a filament-winding process is demonstrated and also materials of filament winding and applications of filament wound products are given. Information and procedure about impact and fatigue tests are given.

Secondly, impact tests and fatigue test results are presented. The impact tests are performed at three different energy levels as 5J, 7.5J, and 10J at room temperature. The impact characteristics such as peak force, maximum deflection and total absorbed energy are listed. The mentioned impact characteristics of both conditions (dry condition and sea water immersion) are plotted against the impact energies. Using of load-deflection and load-time curves the impact properties of filament wound-glass fiber reinforced plastic (FW-GFRP) pipes are discussed for both conditions. Fatigue life cycles of FW-GFRP pipes and graphs of cycle to failure for all test specimens are given. Damage mechanisms (modes) of composite pipes are examined in detail.

The results obtained are evaluated and discussed by using some graphics and images. Generally, two results are deduced. It is confirmed that impact energy brings about reduction of the burst strength of composite pipes. Remarkable other finding is observed that impact and burst strength values of composite pipes which are exposed sea water (three months) are increased a bit.

Keywords: Composite pipes, Impact, Sea water immersion, Fatigue life

DARBELİ YÜKLEMEYE MARUZ KOMPOZİT BORULARDA DENİZ SUYUNUN ETKİSİ

ÖZ

Bu deneysel çalışmanın amacı, darbe hasarı sonrası deniz suyunun kompozit boruların yorulma davranışlarına etkisini araştırmaktır.

Bu çalışmada, ilk olarak, patlama basıncı (yük kapasitesi) ve yorulma ömür çevirimi ile alakalı genel veriler verilmiştir. Filaman sarma tekniği ile kapların üretimi anlatılmıştır. Şematik filaman sarma süreçleri resmedilmiştir. Filaman sargı malzemeleri ve filaman sargılı ürünlerin uygulamaları hakkında bilgiler verilmiştir. Darbe ve yorulma deneyi hakkında bilgi ve prosedürler aktarılmıştır.

İkinci olarak, darbe ve yorulma test sonuçları sunulmuştur. Üç ayrı enerji seviyesine (5J, 7.5J ve 10J) sahip olan darbe testleri oda sıcaklığında gerçekleştirilmiştir. Darbe maksimum kuvvet, maksimum çökme ve toplam absorbe edilen enerji gibi darbe karakteristikleri listelenmiştir. Kuru ortam ve deniz suyu ortamında bulunan numunelerin söz edilen darbe karakteristik eğilimleri uygulanan darbe enerjilerine göre grafiğe dökülmüştür. Yük-çökme ve yük-zaman eğrileri kullanılarak cam filaman sargılı kompozit boruların darbe özellikleri her iki ortam için yorumlanmıştır. Cam filaman sargılı kompozit boruların yorulma ömür çevirimleri ve tüm numuneler için çevrim-hasar fazı grafikleri verilmiştir. Kompozit boruların hasar mekanizmaları (modları) ayrıntılı olarak incelenmiştir.

Elde edilen sonuçlar çeşitli resim ve grafikler yardımıyla değerlendirilmiş ve özgün çıkarımlar yapılmıştır. Genel olarak iki sonuca ulaşılmıştır. Darbe enerjisinin kompozit boruların patlatma mukavemet değerlerinde düşüşe neden olduğu doğrulanmıştır. Dikkate değer diğer bulgu deniz suyuna üç ay maruz bırakılan kompozit boruların darbe ve patlatma mukavemetlerinde bir miktar artış gözlemlenmesidir.

Anahtar sözcükler: Kompozit borular, Darbe, Deniz suyu emmesi, Yorulma ömrü

CONTENTS

Page

CHAPTER ONE
INTRODUCTION

1.1 General View

Fiber reinforced composites become important increasingly in submarine- aircraft vehicles, automotive, sport equipments, weapon-armor industry and so on, this is because fiber reinforced composites are of high specific strength and stiffness.

Pressure vessels, gas and liquid transfer pipes, cryogenic gas tanks, rocket motor cases and launchers manufactured by filament winding methods and loaded by internal pressure are widely used in advanced technologies based on their light-weight, high mechanical properties, damage tolerance, good corrosion resistance and low cost. Variety of parameters for availability is existed for filament wound fiber reinforced plastic (glass; FW-GFRP, carbon; FW-CFRP, aramid; FW-AFRP) pipes such as optimum winding angles, number of layers, volume fractions of fiber, internal pressure and environmental conditions which affect the strength and some other properties (Young modulus, shear modulus, toughness etc.) of the pipes. Background shows that, in generally optimization of composite vessels are done by changing the above-mentioned parameters are investigated.

The FW pipes may be subjected to impact loads due to dropping, pulsating, knocking and/or rough handling. These impact loads cause interlaminar delamination results in reduction in mechanical properties like compression, tension, buckling strength and stiffness of fiber reinforced composites, even the damages are not visible. In this point of view, it is necessary to clarify the strength reduction mechanism after impact and to improve the impact resistance. Also, surface cracks which exist in mentioned composite structures can lead to catastrophical failures, especially in corrosive and cyclic loading conditions.

There are too many investigations, handbooks and articles about composite material. In this study, information about fundamentals of composite materials has

not been acquainted. Therefore the following references are put account for them; Jones R. M. (1999), Mazumdar, S. K. (2002), Mallick, P.K. (2007).

Mightily and adequate studies are done about mechanical behavior of the composite plates. They focused mainly on the mechanical properties like tensile, fatigue, fracture and impact characteristics of the GFRP materials. At the same time, many researchers worked on identifying the effects of impact, consequent delamination, and material properties such as specific energy absorption, maximum peak load, maximum contact time, compressive strength and so on.

On the other hand, it is seen that the effect of dynamic inner pressure (fatigue) on tubes was studied only to a limited extent in recent years. A review of the literature revealed a number of studies focused on pipes but there are fewer investigations about the fatigue and fatigue behavior of fiber reinforced pipes with surface damage (impact, crack etc.). These experimental studies are conducted for several parametric (crack size, crack orientation, exposed matter type etc.) applications.

Experimental studies were main point of this research that aimed to investigate the fatigue behavior of composite pipes after impact damage. The thesis also focuses on the sea water effect failure analysis of composite pipes by experiment. Failure phases of composite pipes are extensively studied.

So that the study generally consist from following three phases experimental test;

1-Expose the specimens 3 months in sea water,
2-Perform various impact loading,
3-Apply dynamic inner pressure (fatigue).

Hydrostatic burst tests were conducted using a self designed an in-house and fabricated HPA corporation. The impact test characteristic was studied by using Ceast-Fractovis Plus impact tester.

In study, researching about the following subject is aimed;

1-Investigate the low velocity impact damage on FW-GFRP pipes,
2-Investigate the effect of sea water sensibility on the low velocity impact damage on FW-GFRP pipes,
3-Observation the damage process during and after subjected to fatigue loading of FW-GFRP pipes,
4-Figure the fatigue cycle to impact energy graph FW-GFRP pipes,
5-Investigate the sea water effect on dynamic loading of FW-GFRP pipes,
6-Predict service life of FW-GFRP pipes under dynamic loading.

1.2 Outline of the Thesis

The structure of this thesis with respect to the main objectives is:

Chapter 2: This chapter provides an introduction to the composite pressure vessels. The general structural efficiency equation of vessels is given and average mechanical properties are compared filament wound composite vis-a-vis others. Physical structure of composite pressure vessels and components are listed, the general data about burst strength and average fatigue life cycle are given. Manufacturing of vessels which is filament winding method is narrated. Schematic of a filament-winding process is demonstrated and also materials of filament winding and applications of filament wound products are given.

Afterward a wide literature review is given that consisted from four subsections; impact damage on composite pipes, burst of composite pipes, burst of composite pipe after damaged and finally effect of water immersion on composite pipes.

Chapter 3: This chapter presents setup of experimental applications of thesis. In this chapter details of specimen, production steps of FW-GFRP pipes, mechanical properties of the fiber and resin are given. It is explicated how is created sea water

simulation and performed impact and fatigue testing. Also detailed figures of experimental setup, equipments and apparatus are given.

Chapter 4: This chapter hosts the main product of the study what the results and discussions. In this chapter, the impact characteristics such as peak force, maximum deflection and total absorbed energy are listed and its trends together comparison of composite pipes both dry and water immersed conditions, against the impact energies. Using of load-deflection and load-time curves the impact properties of FW-GFRP pipes are commented for both dry and sea water immersed conditions.

Cycles of fatigue life of FW-GFRP pipes and graphs of cycle to failure phases of fatigue life of all test specimens are given finally fatigue observations of tubes is listed.

Chapter 5: in this chapter, summation of the results of the impact tests, the fatigue tests and the sea water effect are given. Then related with experiment recommendations is presented.

CHAPTER TWO
COMPOSITE PRESSURE VESSELS AND MANUFACTURING

2.1 Composite Pressure Vessels

Pressure vessels have long been manufactured by filament winding. Pressure vessels appear to be simple structures, but they are among the most difficult to design. Filament-wound composite pressure vessels have found widespread use not only for military use but also for civilian applications. This technology previously developed for the military's internal use was adapted to civilian purpose and following this, extended to the commercial market. Applications include breathing device, such as self-contained breathing apparatuses used by fire-fighters and other emergency personnel, scuba tanks for divers, oxygen cylinders for medical and aviation cylinders for emergency slide inflation, opening doors or lowering of landing gear, mountaineering expedition equipment, paintball gas cylinders, etc. .

A potential widespread application for composite pressure vessels is the automotive industry. Intensions for reducing emissions leads the conversion to Compressed Natural Gas (CNG) fuelled vehicles worldwide. The main aim of the industry here is the attempt to replace fuel oils with natural gas or hydrogen as the energy supply in vehicles for air quality improvements and reduce global warming. The successful application of these fuels in vehicles may be achieved by fuel cells in concert with hydrogen gas storage technologies. One of the missing milestones here is the inadequacy of the vehicle range between refueling stops. Other important parameters in these applications are weight, volume and cost of the containment vessel (Onder, 2007).

Filament-wound composite pressure vessels developed from high strength and high modulus to density ratio materials offer significant weight savings over conventional all-metal pressure vessels for the containment of high pressure gases and fluids. The structural efficiency of pressure vessels is defined as:

$$e = \frac{P_b V}{W} \tag{2.1}$$

where; P_b: Burst pressure, V: Contained volume, W: Vessel weight

The structural efficiencies of all-metal pressure vessels change from $7.6*10^6$ to $15.2*10^6$ mm while filament wound composite vessels have efficiencies in the range from $20.3*10^6$ to $30.5*10^6$ mm. This can be stated as the structural efficiencies of composite pressure vessels are better than all-metal pressure vessels of similar volume and pressure. Also some other properties of tubes are compared below in Table 2.1 (Onder, 2007).

Table 2.1 Property comparisons: Filament wound composite vis-a-vis others (C-K Composites)

Material *	Density (g/cc)	Tensile Strength (MPa)	Tensile Modulus (MPa)	Specific Tensile Strength (10^3 m)
Filament Wound Composite	1.99	1034	31.02	52.96
Aluminium 7075-T6	2.76	565	71.01	20.87
Stainless Steel -301	8.02	1275	199.94	16.20
Titanium Alloy (Ti-13 V-12 Cr-3 Al)	4.56	1275	110.3	28.50

*For unidirectional composites, the reported modulus and tensile strength values are measured in the direction of fibers.

Composite vessels with very high burst pressures (70-100 MPa) are in service today in the aerospace industry. Vessels with burst pressure between 200 – 400 MPa are under investigation and such containment levels were achieved in the late 1970's through mid 1980's. Further researches must be made for the design of advanced ultra-high pressure composite vessels (Onder, 2007).

A maximum pressure of 35 MPa is permitted under current regulations, 21 MPa is a standard vehicle refueling system's nominal output pressure for civilian applications. Higher pressures are not yet approved for use on public roads or

commercial aircraft. This implies a great need for advancement in composite pressure vessel technology (Onder, 2007).

2.1.1 Structure of Composite Pressure Vessels

Cylindrical composite pressure vessels mostly consist of a metallic/plastic internal liner, a filament wound and a composite outer shell as shown in Fig. 2.1. The liner is used to prevent leakage of the high-pressure fluid through the matrix microcracks that often form in the walls of filament-wound fiber-reinforced epoxy pressure vessels. Some of the metal liners also provide strength to share internal pressure load. For composite pressure vessels, a big portion of the applied load is carried by the strong outer layers made from filament wound composite material, and this design of the outer filament wound composite material is mostly the main parameter for the amount of pressure that can be present in the container (Onder, 2007).

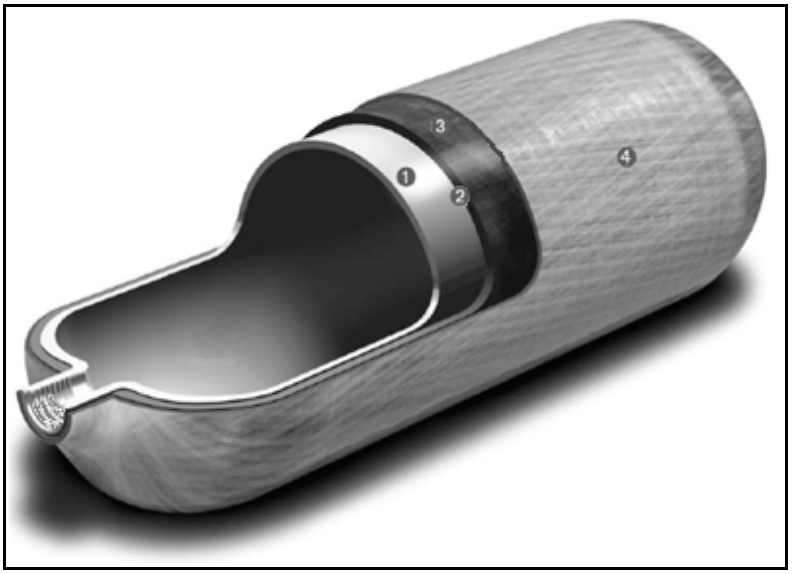

Figure 2.1 Example of universal filament wound composite pressure vessels.

1- Thin plastic liner / Ultra thin-walled aluminum liner
2- Insulating layer
3- High - performance carbon - fiber overwrap in epoxy resin matrix.
4- High - strength glass fiber reinforced plastic (GFRP) protective layer

In the following there are some comments for production process of composite pressure vessels and internal pressure (static and dynamic).

The winding is done on the liner, which also serves as a mandrel. The winding tension and the subsequent curing action create compressive stresses in the liner and tensile stresses in the fiber reinforced epoxy overwrap. After fabrication, each vessel is pressurized with an internal proof pressure (also called the 'sizing' pressure) to create tensile yielding in the metal liner and additional tensile stresses in the overwrap. When the proof pressure is released, the metal liner attains a compressive residual stress and the overwrap remains in tension. In service, the metal liner operates elastically from compression to tension and the composite overwrap operates intension mode (Mallick, 2007).

The internal pressure generates tensile normal stresses in the tank wall in both the hoop (circumferential) and axial directions. The hoop stress for the most part is twice the axial stress. The tanks are designed to withstand a maximum (burst) pressure three times the operating pressure. Selected numbers of tanks are tested up to the burst pressure after subjecting them to 10,000 cycles of zero to operating pressure and 30 cycles of zero to proof pressure. Leakage before catastrophic rupture considered the desirable failure mode during this pressure cycling. Other major qualification tests for the air-breathing tanks are drop impacts, exposure to high temperatures in the pressurized condition, and exposure to direct fire (Mallick, 2007).

2.2 Filament Winding

Filament winding is a fabrication technique for creating composite material structures. The process involves winding filaments under varying amounts of tension over a male mould or mandrel. The mandrels rotates while a carriage moves horizontally, laying down fibers in the desired pattern. In Figure 2.2 schematic of a filament-winding process is shown. The most common filaments are carbon or glass fiber and are coated with synthetic resin as they are wound. Once the mandrel is

completely covered to the desired thickness, the mandrel is placed in an oven to solidify (set) the resin. Once the resin has cured, the mandrel is removed, leaving the hollow final product.

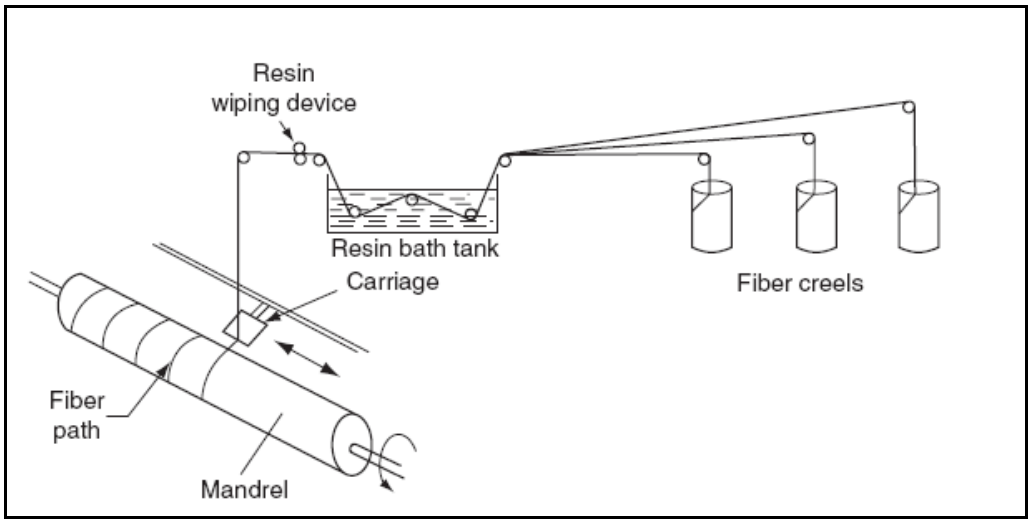

Figure 2.2 Schematic of a filament-winding process (Mallick, 2007).

Filament winding is well suited to automation, where the tension on the filaments can be carefully controlled. Filaments that are applied with high tension results in a final product with higher rigidity and strength; lower tension results in more flexibility. The orientation of the filaments can also be carefully controlled so that successive layers are plied or oriented differently from the previous layer. The angle at which the fiber is laid down will determine the properties of the final product. A high angle "hoop" will provide crush strength, while a lower angle pattern (known as a closed or helical) will provide greater tensile strength.

The mechanical properties of the helically wound part depend strongly on the wind angle, as shown in Figure 2.3.

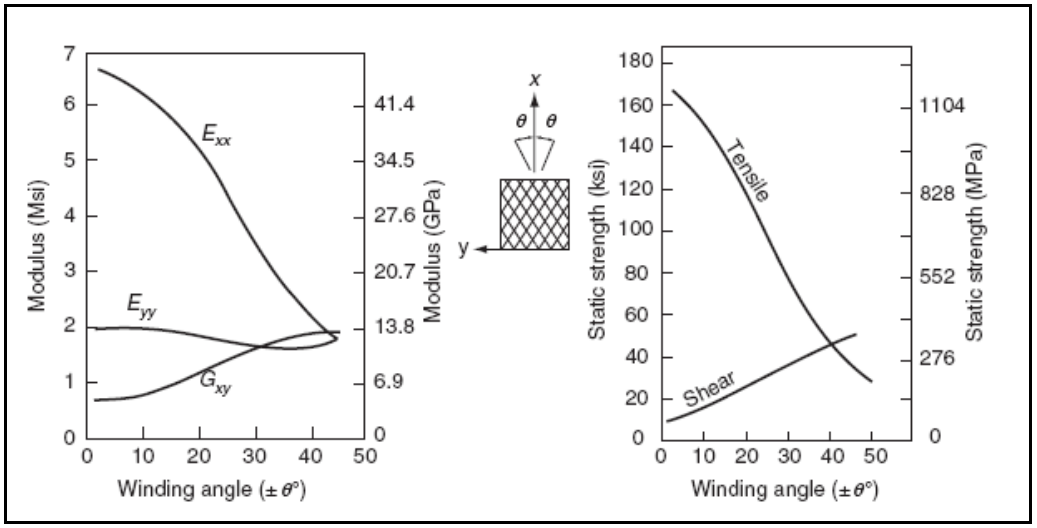

Figure 2.3 Mechanical property variations in a filament-wound part as a function of wind angle (Mallick, 2007).

2.2.1 Materials of Filament Winding

Glass fiber is the fiber most frequently used for filament winding, carbon and aramid fibers are also used. Most high strength critical aerospace structures are produced with epoxy resins, with either epoxy or cheaper polyester resins being specified for most other applications. The ability to use continuous reinforcement without any breaks or joins is a definite advantage, as is the high fiber volume fraction that is obtainable, about 60% to 80%. Only the inner surface of a filament wound structure will be smooth unless a secondary operation is performed on the outer surface. The component is normally cured at high temperature before removing the mandrel. Finishing operations such as machining or grinding are not normally necessary (Filament winding, wikipedia.org).

In Figure 2.4, some filament wound parts and in Table 2.2, applications of filament wound products are given.

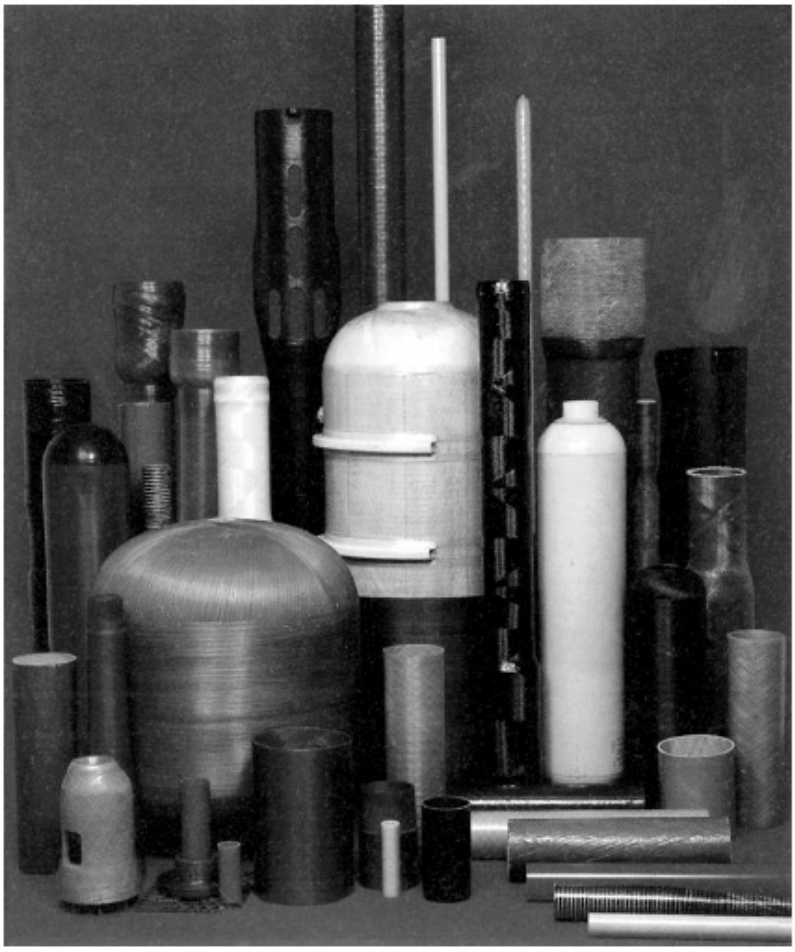

Figure 2.4 Filament wound parts (Mazumdar, 2002).

Table 2.2 Filament wound products: Applications and Resin systems (C-K Composites)

Industry	Typical Application	Typical Resin Systems
Corrosion	•Underground Storage Tanks • Aboveground Storage Tanks	Polyester (Ortho- and Isophthalic), Vinyl Ester
	• Piping Systems • Stack Liners • Ducting Systems	Polyester (Ortho- and Isophthalic), Vinyl Ester, Epoxy, Phenolic
Oilfield	• Piping Systems • Drive Shafts • Tubular Structures	Epoxy, Phenolic
Paper and Pulp	• Paper Rollers • Piping Systems • Ducting Systems	Vinyl Ester, Epoxy
Infrastructure and Civil Engineering	• Column Wrapping • Tubular Support Structures • Power Poles • Light Standards	Polyester (Ortho- andIso-phthalic), Vinyl Ester, Epoxy
Commercial Pressure Vessels	• Water Heaters • Solar Heaters • Reverse Osmosis Tanks • Filter Tanks • SCBA (Self-Contained Breathing Apparatus) Tanks • Compressed Natural Gas Tanks	Polyester (Ortho- and Iso-phthalic), Vinyl Ester, Epoxy
Aerospace	• Rocket Motor Cases • Drive Shafts • Launch Tubes • Aircraft Fuselage • High Pressure Tanks • Fuel Tanks	Epoxy, Bismaleimide (BMI), Phenolic, Vinyl Ester
Marine	• Drive Shafts • Mast and Boom Structures	Epoxy
Sports and Recreation	• Golf Shafts • Bicycle Tubular Structures • Wind Surfing Masts • Ski Poles	Epoxy

2.3 Background

Many studies on GFRP degradations are reported in the literature that includes corrosion, electromagnetic effects, fatigue, water immersion, fire, impact damage, weathering, temperature, rain erosion etc. Among them, three major effects (impact damage, fatigue, water immersion) is investigated on that could significantly degrade GFRPs are.

This literature review has consisted from four subsections; the impact damage on composite pipes, the burst of composite pipes, the burst of composite pipes after damaged and finally the effect of water immersion on composite pipes. So that background of this thesis divided four subheadings.

2.3.1 The Impact Damage on Composite Pipes

Composite materials are very sensitive to out-of-plane loading (i.e., loading transverse to plies or reinforcement) because they are much weaker in the thickness direction than in the plane of lamination. Consequently, composite materials subjected to transverse impact may suffer significant damage, resulting in deterioration of its overall load-carrying capacity. The response of composite materials to these impact loadings is complex, as it depends on the structural configuration as well as the intrinsic material properties. Further, it depends on the material, geometry, and velocity of the impactor (Naik, 2005).

Each plays an important role in characterizing the overall effect of transverse impact. The various forms of damage modes possible under impact loading range from non-visible or barely visible to penetration of the impactor. Low velocity impacts may not cause any visible damage on the laminate but may cause internal damage in the form of matrix cracking, delamination, and/or fiber cracking inside the laminate. This may lead to significant reduction in strength. Stiffness reductions are also possible but not generally dramatic. A common example of low velocity impact is the accidental dropping of a tool on the composite

component or structure during manufacturing, service, or maintenance. Generally, impact with impactor speeds less than 100 m/s are classified as low velocity impact. But there are several other definitions of low velocity impact, with no universal agreement. Sometimes low velocity impact is used in the context of low energy impact, i.e., less than 136 J (100 ft-lb). Low velocity impact normally involves deformation of the entire structure during the contact duration of the impactor, and this situation is considered quasi-static with no consideration of the stress waves that propagate between the impactor and the boundary of the impacted component. On the other hand, high velocity or hypervelocity impacts involve impactor speeds greater than 1 km/s. This is sometimes also referred to a situation where complete penetration of target (i.e., composite structure) occurs. Usually, the deformation of the composite structure in high velocity impact is localized in a small zone surrounding the contact area during the duration of contact with the impactor (Naik, 2005).

To simulate actual impact by a foreign object, a number of impact test apparatuses are suggested: Gas gun apparatus, drop weight tester, cantilevered impactor, and pendulum-type tester. In his book “Impact on Composite Structures”, Abrate (1998), has introduced the articles describing these impact test apparatus. Of these apparatus, drop weight tester, and gas gun are used by most investigators. Although much detail of the actual test apparatus may differ, schematic illustrations of these apparatuses including main parts are given in Figure 2.5 (Atas, 2004).

In experimental studies it is attempted to replicate actual situations under controlled conditions. Even if the initial impact energies of the projectiles are exactly the same, a smaller mass with higher initial velocity and a large mass with low velocity may cause different amount of damage and damage modes. Therefore, type of apparatus chosen and impact factors affecting the response of the structure, such as velocity of the projectile, gain high importance in experiments. For example, dropping of tools on the structures during maintenance operations can be simulated by drop weight tester while flying of debris on the runway during

aircraft takeoffs or landings can be best simulated using a gas gun with small high velocity projectiles (Atas, 2004).

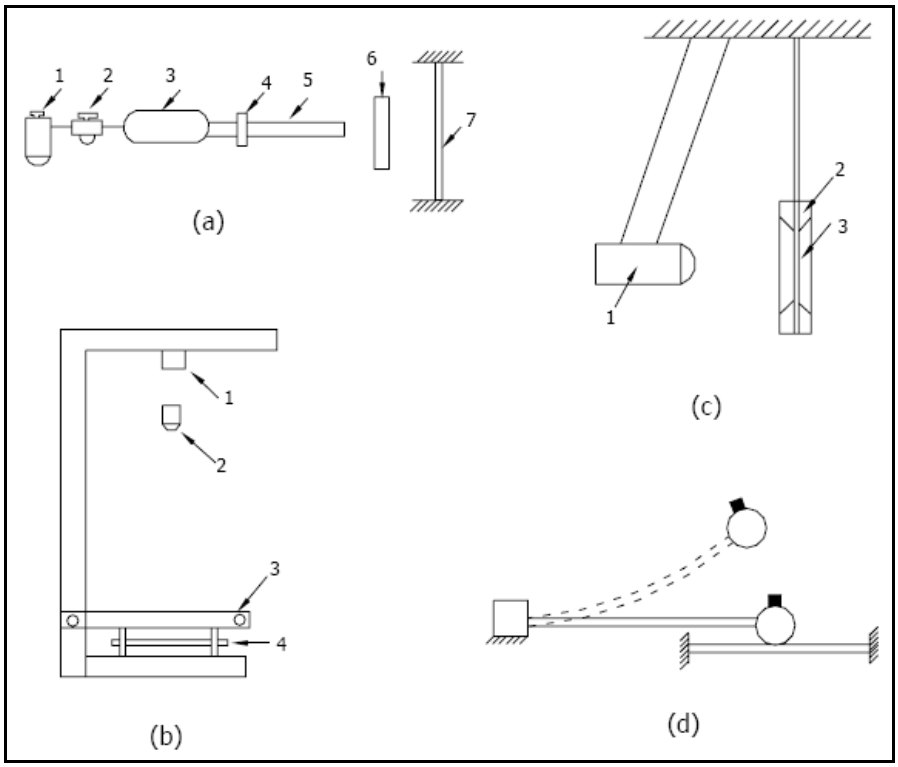

Figure 2.5 Types of impact test techniques (Abrate, 1998). (a) Gas gun apparatus: 1-air filter, 2-pressure regulator, 3-air tank, 4-valve, 5-tube, 6-speed sensing device, 7-specimen; (b) Drop weight tester: 1-magnet, 2-impactor, 3-holder, 4-specimen; (c) Pendulum-type tester: 1-impactor, 2-specimen holder, 3-specimen; (d) Cantilevered impactor.

Type of the test apparatus and other impact parameters such as projectile characteristics were not of high importance in this study. There are some specific terms which using on impact tests. These are listed below.

The peak load is the maximum contact force between the impactor and the composite at the contact point. Contact duration is determined as the total time of contact. The maximum deflection of a composite is defined as the largest depth on the top surface from the initial position to deflected position for non-perforated specimens and it is defined as the deflection up to the perforation point for the

perforated specimens. The absorbed energy is the energy consumed between the impactor and the specimen through the formation of damage and friction.

Currently, however, increasing use is being made of instrumented impact tests with drop weight impact testers to characterize the low velocity impact of composite structures. This is usually done on drop weight impact machines, where the striker is instrumented to measure the applied load. These machines have means of measuring displacement or acceleration. Thus the history of the load, displacement, and acceleration during the impact event is recorded, and these can be converted to give impact load-time and impact energy-time histories. From these, features such as peak load and absorbed energy can be related to fracture processes occurring in the material. A typical load history in an impact test is schematically shown in Figure 2.6. The load-time history can be divided into two distinct regions, a region of fracture initiation and a region of fracture propagation. As the load increases during fracture initiation phase, elastic strain energy is accumulated in the specimen and no gross failure takes place; but failure mechanisms on a microscale for example, microbuckling of the fibers on the compression side or debonding at the fiber-matrix interface are possible. When a critical load is reached at the end of the initiation phase, the composite specimen may fail either by a tensile or a shear failure depending on the relative values of the tensile and interlaminar shear strengths. At this point the fracture propagates either in a catastrophic "brittle" manner or in a progressive manner continuing to absorb energy-at smaller loads (Naik, 2005).

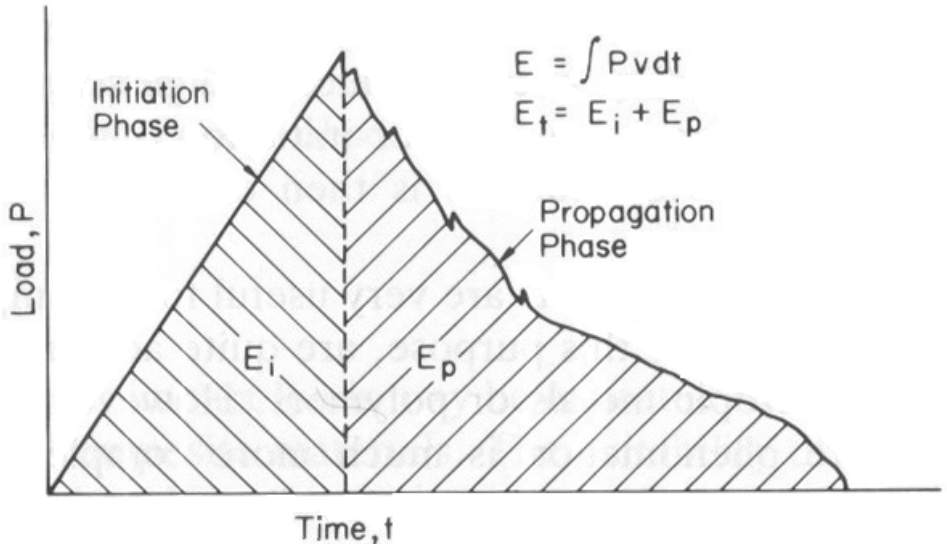

Figure 2.6 Typical load history during impact test. (Shyr & Pan, 2003)

The total impact energy, E_t as recorded on the impact machine or on the energy-time curve on the oscilloscope is thus the sum of the initiation energy, E_i and propagation energy, E_p. A high-strength brittle material which has a large initiation energy but a small propagation energy and a low-strength ductile material which has a small initiation energy but a large propagation energy-may have the same total impact energy (Naik, 2005).

It has being seen that impact on tubes was studied only to a limited extent in recent years. There were investigations about burst strength reduction after surface damage (impact, indentation or surface crack) on FW-GFRP, FW-CFRP and FW-AFRP pipes (with/without “liner”).

Some researchers worked on identifying the effects of impact, consequent delamination, and material properties such as specific energy absorption, maximum peak load, maximum contact time, compressive strength and so on.

Doyum & Altay (1997) focused on the detection of damage after low velocity transverse impact loading on thin FW-GFRP (E- and S-glass) pipes experimentally. They used visual inspection and post emulsified fluorescent penetrant systems for damage detection and presented types and characteristics of defects.

Karbhari, Haller, Falzon & Hersberg (1999) investigated post-impact crush of FW-GFRP, FW-CFRP, FW-AFRP and hybrid pipes which were different layer. They showed that impact damage causes a reduction in the specific energy absorption of FW pipes.

Zou, Reid, Li & Soden (2002) developed a new model for progressive interlaminar delamination of laminated composites (FW-GFRP). They used a stress-based failure criterion for estimation of delamination initiation and fracture mechanics approach for propagation of delamination. In addition, this analysis has included matrix cracking which is significant intralaminar damage mode. They determined deformation and delamination of laminated composite structures with finite element analysis (FEM). Test specimens had two orientations and two radiuses. Results of the studies on mesh size of the FEM model showed that even relatively coarse mesh size gives enough exactly results. Experimental and FEM results were accorded. Hereby, it has being seen Zou et al.'s results are available real structural applications.

Chib (2003) studied on simulating the response of low velocity impact test on FW-CFRP pipes with finite element software LS-Dyna. In addition, parametric studies such as impactor velocity, lay-up configurations and boundary conditions of composite pipe etc. which affect the impact damage process were investigated. The model of impact test was illustrated and the mentioned parametric test results were shown up. The result of parametric (numeric) analysis was compared with experimental results. Study of Chib verified the validity and effectiveness of finite element simulation, because results of simulation had great similarity of experimental test and predicted good simulation.

Changliang, Mingfa, Wei & Haoran (2006) studied on low velocity impact kinetic theory for the composite hybrid which is laminated with metal liner vessel. FEM is used to investigate the impact response of composite pipe with and without internal pressure and predict their damage distributions during and after impact. They

considered the damage styles-damage distributions of different impact velocities, geometric and material nonlinearities and the effect of contact in the analysis. They noticed that the impact damage extent for composite FW vessel with internal pressure is more severe than that without internal pressure under low velocity impact case with same kinetic energy.

Tarfaoui, Gning, Davies & Collombet (2007) investigated on dynamic response and damage characteristics of composite pipes. They aimed at improvement of understanding the scale effects on the behavior of composite tubular structure for the design of underwater equipment. With the results of the test, they commented that "Although the damage is of comparable nature for all the tubes, it was necessary to establish particular laws of similitude in order to predicted the damage of a model cylinder from that of the prototype and vice versa". The tests show that the response of the structure has the primary importance in establishing the balance between elastic deformation and local damage development.

Secondly, Tarfaoui, Gning & Hamitouche (2008) investigated finite element analysis of static and dynamic tests on thick FW-GFRP pipes to improve the long-term integrity of composite structures for underwater applications. The study consists of two parts. First part is the validation of elastic properties and identification of damage initiation and its development in dynamic tests and second part is an impact model, including material property degradation, used for damage prediction. Analytical models and finite element analysis are presented on text. The study showed that there is a strong relationship between the structure and material. They have expressed that it is important to control the influence of the conditions of development on the limiting values of material.

2.3.2 The Burst of Composite Pipes

Hydrostatic testing is universally known and accepted as a means of demonstrating the fitness of a pressurized component for service. After a test, a pipeline or pressure vessel can be expected to safely contain its intended operating

pressure. The confidence level that a pipeline or pressure vessel is fit for safe service increases as the ratio of test pressure to operating pressure increases. This highly beneficial aspect of hydrostatic testing applies not only to a new component to be placed in service for the first time. A similar benefit accrues to an in-service component if that component is taken out of service after a period of time and subjected to a hydrostatic test. A “revalidation” test of the latter type assures either that no significant time dependent deterioration of the component has taken place or that any segment that is significantly degraded will be revealed and eliminated (Naik, 2005).

A test reveals weaknesses by causing ruptures or leaks; it does not indicate, for example, other areas where active corrosion may be taking place. A limitation that has both technical and economic implications is that a level of test pressure to operating pressure sufficient to generate high confidence may result in numerous test breaks or leaks. Repeated test failures may actually reduce confidence in the final margin of safety demonstrated by the test, and such failures will certainly add significantly to the cost of the test and the time out of service.

The pressure required to result in such a failure is known as the 'burst pressure'. Actual pipe samples are pressurized with water as the internal medium and either air or water as the external medium. The internal pressure in the pipe samples results in both an axial and a hoop stress. As the hoop stress is twice the axial stress, it is the stress in the hoop direction that results in failure. The hoop stress is given:

$$\sigma_h = \frac{Pr}{t} \tag{2.2}$$

$$\sigma_a = \frac{Pr}{2t} \tag{2.3}$$

where; σ_h: Hoop stress, σ_a: Axial stress, P: Inner pressure, r: Radius, t= Thickness

> In the literature, the optimum winding angle for filament wound composite pressure vessels is given as 54.74^{o} by netting (meshing-optimize) analysis. …. Here, it is clear that the more the fiber orientation is changed from 55º, the more the first-ply failure pressure drops (Yaylagan, 2010).

Sun, Du & Wang (1999) investigated on solid-rocket motor cases which are a kind of composite structure by using the nonlinear FEM. They have worked up to detect the effects of material performance and geometrical nonlinearity on the relative loading capacity of the dome. So, they have calculated the stresses and the bursting pressure of aforementioned vessel. From the view point of burst, the design method from the analogous case to its real one is not rational. Because in the model I case, the conclusion obtained was contrary to that for the model II case without skirts. They decided that all affecting factors should be considered synthetically to obtain the optimum structure.

Chang (2000) studied via the first-ply failure strength on symmetrically laminated composite pressure vessels with various material properties, radius-to-thickness ratios, and different numbers of layers subjected to uniform internal pressure loads by experimental and analytical approaches. Optimal angle-ply orientations for maximum stiffness were investigated. A comparison between the experimental approaches and the analytical methods was made to demonstrate the suitability of the failure criteria in predicting first-ply failure strength. In particular, the Hill criterion can predict first-ply failure pressure load with error around 1%.

Kim, Kang, Hong & Kim (2005) aim to establish an optimal design method of FW structures under internal pressure. In this research, the semi-geodesic path algorithm was used to calculate possible winding patterns taking into account the windability and slippage between the fiber and the mandrel surface. In addition, progressive failure analyses were performed to predict the behavior of FW structures on ABAQUS. In particular, suitable element types and failure criteria for FW structures were studied. Finally, the developed design code was applied to a symmetric composite pressure vessel for verification.

Zheng & Liu (2008) concentrates on a theoretical model of the composite cylindrical laminates under internal pressure and thermal residual stress. The theoretical model based on the last ply failure criterion, a solution algorithm is further presented to explore the damage evolution and the burst strength of the structure. Effects of the winding angle and number of the composite layers as well as the thermal residual stress are explored. They calculated burst strengths and also compared with the experimental results hence the calculated burst strengths are in good agreement with the experimental results. The tests show that the thermal effect increases the radial, hoop and axial stresses in the winding layers, but decreases the hoop and axial stresses in the liner. Secondly, with increasing winding angle, the radial displacement and shear–stress decrease, but the radial stress increases.

Khalid, Hamed & Sapuan (2007) is investigated bursting pressure and the carrying capacity of basic plastic tubes, composite tubes and reinforced plastic tubes under internal pressure. They exposed of the effect of the material type as filament winding and woven roving and the effect of number of layers by experimentally.

Onder, Sayman, Dogan & Tarakcioglu (2009) examined on the influences of temperature and winding angle on FW-GFRP pipes for increasing the maximum burst pressure. Burst pressure of FW composite pressure vessels under alternating pure internal pressure was investigated. The hygrothermal and other mechanical properties were measured on E-glass–epoxy composite flat layers. Some analytical and experimental solutions were compared with the finite element solutions about verifying the optimum winding angles. Finally they appointed that the burst pressure of the composite pressure vessels varies at high temperatures, since the strength of the composite material decreases and thermal stresses occur at the high temperatures.

In addition, Onder, (2009) is proved that related production steps of this composite pressure vessel design approximately 20ºC application environment as the best application temperature value.

Velosa, Nunes, Antunes, Silva & Marques (2009) investigated on FW-GFRP vessels with thermoplastic liner in their article which is part of a larger study concerning the development of a new generation of FW composite vessels to be applied on the storage of industrial uncompressed fluids under pressure. They used FEM to predict the mechanical behavior of pressure vessels. Finally, prototype pressure vessels were produced and submitted to pressure tests in similar conditions to those used in the FEM simulations. Experimental results obtained on the produced composite prototype vessels under internal pressure test confirmed the burst pressure values obtained from FEM calculations.

Xu, Zheng & Liu (2009) studied on parametric finite element model of the cylindrical part of composite hydrogen vessel (FW-CFRP with Al liner) to explore the non-linear stress–strain relationship and the final failure. They aimed to find the progressive damage and failure properties of mentioned composite structures with increasing internal pressure. The failure pressures (for different failure criteria) are compared with the experimental burst pressure of composite hydrogen storage vessels. By comparison, the failure pressure using the proposed FEM's are in agreement with the experimental burst pressure of composite vessel. However, the Tsai–Wu failure criterion leads to most accurate failure pressure among all failure criterions.

2.3.3 The Burst of Composite Pipes After Damaged

Tarakcioglu, Akdemir & Avci (2001) investigated on the effect of surface cracks on strength for FW-GFRP pipes with analytically and experimentally. They set the specimens three different orientations with surface crack which have several notch-aspect ratios and notch-to-thickness ratios in the axial direction. They determined critical stress intensity factors and compared the strength values of pipes with surface cracks are with internal pressure test results and theoretical results.

Curtis, Hinton, Li, Reid & Soden (2000) investigated the damage, deformation and residual burst strength of FW-GFRP pipes subjected to impact/quasi-static

indentation numerically and experimentally. They found that the behaviors of pipes subjected to quasi-static and low velocity impact loading tests were same. Experimental strain measurements in quasi-static indentation tests showed a large degree of redistribution of strain with increasing deflection which resulted in local buckling failure away from the indentation point. Damage in the form of matrix cracking resulted from low energy indentation but did not reduce the residual burst strength of the pipe. Low speed impacts caused the pipes to fail by local axial shell buckling, leading to local delamination and fracture some distance away from the indenter. That failure reduced the residual burst strength by about 60% from 10 to 4 MPa.

Naik (2005) realized great experimental priming on his master thesis that involved many different effects of environmental conditions such as sea water immersion, dry heat, salt spray, humidity and impact on the burst pressure performance of the glass fiber reinforced thermoset pipes (glass-epoxy and glass vinylester). He calculated and illustrated the failure pressures for different impact energies and residual pressure strength ratios. It can be seen that the residual strength tends to decrease with increasing impact energy delivered to the pipes. He also characterized a typical curve of residual strength vs. impact energy by three main regions, which can be identified by the gradient of the residual strength curve. The test showed that; at relatively high impact energies, where the impact damage zones was relatively large and the failure occurred by weeping. Low impact energies, where the impact damage zone was small, leakage, weeping or burst occurred from regions located generally circumferentially 90° away from the impact zone or on the opposite side (180°) to the impact damage zone of the GFRP pipe.

Arikan (2010) studied on the failure analysis of FW-GFRP pipes with an inclined surface crack, numerically and experimentally. Tests are performed at seven different crack angles: 0°, 15°, 30°, 60°, 45°, and 75°. Arikan determined the burst strengths of the specimens and examined the dependence of the burst strength on the crack angle. He listed these determinations; Examination of the crack zone has revealed that the crack growth started with delamination. The failure band was formed by an

increase in delamination. After the separation of the band, failure ended with sudden seepage at the crack zone. That is, cracks parallel to the fibers started several millimeters from the interlaminar zone located on the fiber bundle crossing, leading to seepage. As a result of the study, the influence of inner pressure on failure modes and the impulse, work, and load at penetration were studied and the relationship between burst mode and inner pressure can be clarified.

The gradual studies are conducted by group of Department of Mechanical Engineering in University of Manchester on improving the long-term integrity of composite structures for underwater applications. In all three studies, same FW-GFRP pipe are used. Some indications of how this damage affects the capacity of cylinders to resist external pressure loading were also presented their article. They noticed that the impact damage is shown to reduce the residual implosion strength of FW-GFRP pipes significantly.

Gning, Tarfaoui, Collombet & Davies (2005) showed the experimental results obtained from quasi-static and impact indentation tests on FW-GFRP pipes intended for underwater applications. In their study, they performed following acts. Drop weight impact tests was performed on thick pipes at energies up to 45 J; ultrasonic inspection was employed first to determine projected damage areas; a large number of samples were then sectioned and polished and the true damage area was revealed by a dye penetrant technique. The influence of impact damage on implosion pressure was described. Above a critical impact energy level a significant drop in implosion resistance was noted, which is related to the appearance of intralaminar cracks. Low impact energies resulted in a large drop in implosion pressure resistance. According to test results; Impact damage has promoted a local implosion failure mechanism. Damage in static indentation is similar to that noted in impact tests but the damage dimensions are not identical. Finally; modelling of damage development and its influence on implosion pressure is performed in parallel with the experimental studies presented.

Gning, Tarfaoui, Collombet, Riou & Davies (2005) investigated the identification and modeling of damage initiation and development in glass-reinforced epoxy composite cylinders subjected to drop weight impact. In their article, some indications of how this damage affects the capacity of pipes to resist external pressure loading were also presented. They noticed that the impact damage is shown to reduce the residual implosion strength of glass/epoxy cylinders significantly. A 12-J impact reduces the implosion pressure by 40%. This provides a great incentive for the development of structures with improved damage tolerance.

Tarfaoui, Gning & Collombet (2007) is resulted from static and dynamic tests on FW-GFRP pipes. The first part involves the identification of damage initiation and its development. Second part of the article is concerned with the evaluation of the influence of this damage on residual strength under hydrostatic pressure loading. The results show a threshold effect, even for damaged cylinders, which indicates a certain tolerance to the damage. The damage influence becomes more important as the energy of impact increases. The reduction of the residual strength behavior does not evolve regularly as a function of the damage in the tubes.

Chang (2003) investigated with numerical and experimental the failure modes of undamaged and damaged composite pipes subjected to internal pressure and to qualitatively determine the relative burst pressure degradation. Pipes were intentionally damaged by either a longitudinal-line cut or a single-point impact. Both types of damage were intended to simulate fiber breakage caused by a local damage. Testing was conducted under three conditions: hydraulic pressurization, pneumatic pressurization with solid inserts, and pneumatic pressurization with inert propellant inserts. A pipe with a longitudinal cut can fail by three different modes: a local leakage mode, a bursting mode with fracture initiating from the cut, or a bursting mode with complete pipe disintegration. In testing of impact-damaged pipes, the results show that the burst pressure decreases with increasing impact load. At an impact load of 1493N the burst pressure decreases by 33% compared to the undamaged condition.

Kaneko, Ujihashi, Yomoda, & İnagi (2008) studied on the impact analyses of pressurized FW-CFRP vessels by simulation. He the impact analyses with the general FE analysis code ‘‘LS-DYNA’’ and showed the qualitative validity of model and considered relationships between inner pressure, thickness and failure mode.

In addition, on same theme, some studies are revealed about FW-CFRP pipes with Aluminum liner.

Wakayama, Kobayashi, İmai & Matsumoto (2002) investigated to improve the residual burst strength of FW-CFRP composite pipes after impact loading, three types of low-modulus pitch-based carbon fiber with high-compressive strain to failure were wound on the surface of the pipes. Impact and internal pressure tests were conducted on the specimens to evaluate the effectiveness of the low-modulus pitch-based carbon fiber. Impact damages, which consist of fiber damage and delamination, were evaluated as functions of impact conditions to clarify the failure mechanism of these specimens. The test showed that the residual burst strength ratio decreased linearly with increasing effective damage depth ratio considering the contribution of the each plies to the burst strength. Consequently, it is clarified that the residual burst strength was enhanced with the application of the low-modulus pitch-based carbon fiber.

Kobayashi, İmai & Wakayama (2007) studied on elasto-plastic analysis on the filament-wound carbon fiber-reinforced plastic (FW-CFRP) hybrid composite pipes subjected to internal pressure was proposed. They investigated to predict burst strength of the FW-CFRP hybrid composite pipes and residual strength after impact based on the maximum strain criterion and compared the result experimentally. The stress distributions calculated based on the present analysis are in good agreement with the FE results. The analytical results are consistent with the experimental results in case of the lower deformation of the composite pipes.

Long-term data on glass-fiber reinforced polymeric composites subjected to cyclic loading has not been well documented and is still poorly understood. During the

fatigue test, four damage modes were typically observed at various stages of the test: transverse matrix cracking, delamination, fiber/matrix debonding and fiber fracture. While matrix cracking and delamination occur early in the test, the latter two damage modes typically initiate and develop rapidly towards the end of life (Naik, 2005).

A review of the literature revealed a number of studies focused on pipes but there were fewer investigations about the fatigue and fatigue behavior of fiber reinforced pipes with surface crack. Experimental studies are conducted about the fatigue behavior of FW-GFRP pipes with varieties of parametric applications.

Samanci, Avci, Tarakcioglu & Sahin (2008) studied on fatigue damage behavior of FW-GFRP pipes with different surface cracks under alternating internal pressure. The failure behavior of GRP pipes during the test was observed and fatigue test results were presented by means of (S–N) curves and delamination damage zone area-cycle (A–N) curves. The effect of notch depth-to-thickness ratios and hoop stress level ratios were investigated. The relationship between delamination areas versus fatigue cycle (A–N) was also investigated. At high stress the delamination propagation rate decreased quickly and then propagation stopped, while at low stress delamination saturation takes much more time, and cycles to delamination saturation decreased considerably with increasing a/t ratio.

Tarakcioglu, Gemi & Yapici (2005) investigated fatigue behavior of filament wound composite pipes under alternating internal pressure is investigated experimentally. GRP pipes which made of E-glass/epoxy are tested under open ended conditions. Tests are performed at different load levels from 30% to 70% of ultimate strength. Whitening (fiber/matrix interface debonding and delamination), leakage and final failure levels of GRP pipes are observed. For each damage stage S–N curves were found. There was no evidence of a fatigue limit under the frequencies and stress evaluated. The applied stress ratio had a change in the leakage curve, ranging from a burst type of leakage to slow leakage initiation with a slow increase in the leakage rate until rapid leakage.

Tarakcioglu, Samanci, Arikan & Akdemir (2007) investigated the fatigue behavior of FW-GFRP pipes with a semi-elliptical surface crack. In addition, in these tests, they investigated effects on fatigue failure behavior of sizes of surface crack and applied hoop stress levels. Also, delamination area versus fatigue cycle (A–N) was plotted. The fatigue tests showed that the failure only occurred at the region where the surface crack cuts a glass fiber. This failure did not exceed the crack length, 2c or the boundary of ±55° winding angle. Crack propagation effectively occurred in Mode II.

Gemi, Tarakcioglu, Akdemir & Sahin (2009) investigated the fatigue failure behaviors of FW-GFRP pipes under pure internal pressure. Tests are performed at different load levels from 30% to 70% of ultimate tangential strength of the pipe. The damage progression such as whitening, leakage and final failure are observed, and S–N curves of these damages were obtained. Whitening, leakage and final failure levels of FW-GFRP pipes were observed, and the results obtained were presented by means of S–N curves. They observed that when the applied load is high, the leakage and final failure coincide, whereas when the applied load is low, the leakage is followed by the final failure and it is concluded that at high loads, the fiber failure is important and controls the final damage, while at low loads, the failure is controlled by matrix damage.

Avci, Sahin & Tarakcioglu (2007) examined the corrosion fatigue behavior of FW-GFRP pipes with a surface crack under alternating internal pressure. The surface notches were formed on the outer surface of the pipe along the pipe axis. Dilute (0.6 M) HCl acid was applied to the surface crack region by a corrosion cell mounted on the outer surface of the pipe. It is observed that the surface crack grows through the thickness of the pipe in a planar form. At the end of crack growth process, the pressurized oil leaks from the surface crack as small amounts of oil drops. The variation of the crack growth rates and the stress intensity factor ranges shows a linear relationship and the crack growth rates increase while the crack grows and stress intensity factor ranges increase. The surface crack shows a tendency to change its form to penny shaped. Microcracks are formed on the surface of the glass

reinforcement during corrosion fatigue process and the corrosion fatigue cracks grow as steps.

Sahin, Akdemir, Avci & Gemi (2008) investigated the effect of winding angle upon corrosion fatigue crack growth behaviors of the FW-GFRP pipes with surface cracks, under pure internal pressure subjected to 0.6M HCl acid. The variation of the crack growth rates and the stress intensity factor ranges are showed a linear relationship and the crack growth rates increase while the crack grows and stress intensity factor ranges increase. The fatigue crack growth was smooth even though the crack is across the layer. Two different regions are seen upon the fracture surfaces of the fibers, namely corrosion dominated fracture regions and mechanically dominated fracture regions.

On the other hand Bie, Li, Liu, Liu & Xu (2009) investigated the fatigue evaluation model which is associated with the finite element analysis is proposed to explore the fatigue lifetime of FW-CFRP hydrogen storage vessel under cyclic internal pressure. The fatigue lifetime and S–N curves, numerical results are also compared with the experimental results. The searchers noticed that the fatigue lifetime is relevant to the loading amplitude, mesh size, crack density and practical stress status at the liner.

2.3.4 The Effect of Water Immersion on Composites

Pipes are often in contact with water either due to weathering by rain or by carrying moisture containing fluids and chemicals. Vinylesters containing the ester group in their chain molecules are susceptible to hydrolysis of the side group, which might lead to cross-linking. Water has potentially degrading effect on matrix materials. Moisture in many of its forms-acidic, basic, neutral are known to affect the durability of composites. Moisture present in many forms and eventually penetrates all organic materials by a diffusion controlled or by instantaneous absorption until the moisture equilibrium concentration is achieved. Usually the moisture concentration increases initially with time and finally

approaches the saturation point (equilibrium) after several days of exposure to humid atmosphere. The time to reach the saturation point depends on the thickness of the composite and the ambient temperature. Drying can reverse the process but may not result in complete attainment of original properties. The uptake of water by polymer composites in general follows the generalized Fick's law of diffusion (Naik, 2005).

Liao, Schulthelsz. & Hunston (1999) simulated the pultruded glass-fiber reinforced polymer (GFRP) coupons which aged in several different conditions that common outdoor environment. The tensile and flexural properties were determined after these exposures. The effects of environmental aging on each of the constituents (the fiber, the matrix, and the fiber/matrix interphase region) were studied. As a result, both strengths and moduli were generally found to decrease with environmental aging.

Gellert & Turley (1999) examined ageing behavior which accompanied the sea water immersion of four different composite laminates (isophthalic polyester, a developmental resole phenolic and two vinylester GRP). Water uptake behavior for the GRPs and neat matrix resins, the mechanical properties from flexural and interlaminar shear testing, and creep behavior are reported for laminates which were immersed in a loaded or unloaded condition in the laboratory. As a result, flexural strength fell by 15–21% for the water saturated polyester and vinylester GRPs, and by 25% for the phenolic GRP. Loading at 20% of ultimate strain while under immersion exacerbated only the phenolic laminate degradation, advancing the loss in strength to 36%. Interlaminar shear strengths fell by between 12 and 21% for the GRPs at close to saturation.

Davies, Mazeas & Casari (2001) examined to what extent distilled water accelerated aging can be used to simulate the behavior of typical marine composites in sea water and how the shear behavior of composites with different matrix resins is affected by aging. Additionally they assessed the applicability of damage mechanics parameters to follow wet aging of marine composites. They aged them and to

recorded their weights for a long period of time (over 18 months) and then tested their mechanical properties. (They used an original application of damage mechanics parameters to quantify the changes in composite shear behavior, in order to provide a more complete representation of the inelastic response.) The test showed that, a large part of the shear property lost after aging is recovered after drying.

Davies, Riou, Mazeas & Warnier (2005) investigated FW-GFRP and FW-CFRP pipes for underwater applications. They described simple mechanical and sea water aging screening tests on flat specimens. Cylinders of both were manufactured and subjected to hydrostatic pressure tests, and results are compared to those for glass/epoxy and carbon/epoxy cylinders of similar geometry. According to test authors the FW-CFRP pipes appeared most promising. It resisted pressures in excess of 90 MPa and was retained for damage tolerance assessment studies. Drop weight impact damage zones were smaller in carbon/PEEK than carbon/epoxy for the same impact energies but the loss in residual collapse strength was more rapid in the thermoplastic composite. This was attributed to a change in failure mode; impact damage initiated a local buckling failure.

Kootsookos & Mouritz (2004) investigated the effect of sea water immersion on the durability of FW-GFRP and FW-CFRP composites were experimentally. The materials studied were glass/polyester, carbon/polyester, glass/vinyl ester and carbon/vinyl ester composites used in marine structures. When immersed in sea water at a temperature of 30 °C for over two years, it is seen that the composites experienced significant moisture absorption and suffered chemical degradation of the resin matrix and fiber/matrix interphase region. The mass change is compared between the composites, and the mechanisms responsible for differences in the durability behavior between the materials are investigated. In addition, the effect of water absorption on the fiber/resin interphase region is examined using scanning electron microscopy and mode I interlaminar fracture testing. The effect of sea water immersion on the flexural stiffness and strength of the composites is also determined. It is found that fiberglass composites absorb more moisture than carbon fiber composites, and this may be due to the emulsion size used on glass fibers facilitating

greater water absorption at the fiber/matrix interphase than the silane size on carbon fibers. The mode I interlaminar fracture toughness of the composites was not affected significantly by sea water immersion, although the flexural stiffness and strength decreased with increasing amounts of water absorption.

Gu & Hongxia (2007) investigated the effect of water immersion on the tensile strength and bending behavior and degradation mechanism of the composites experimentally. They put laminates into a distilled water tub. The water uptake was measured for each period. Then they tested the tensile strength and the bending behavior of the samples. It is revealed that as the immersion time of the composites increased, the tensile strength of the specimens was gradually reduced, on the other hand, the bending strength was increased and reasons were analyzed. When the glass/polyester composites are immersed in the water, water uptake would happen. This is the results of capillarity of the materials and the water absorption of the hydrophilic groups in the glass fiber and the unsaturated polyester. The weight uptake would increase with prolonged immersion time as far as the composite is unsaturated. The reaction between the water molecules and the matrix would deteriorate the interphase resulting in a weaker material. The bending resistance showed an increased trend with increased water immersion time. The author believed that the entered water may act as a plasticizer making the laminate a more entirety.

Gu & Hongxia (2008) aimed to find out the bonding behavior between the layers after water immersion. They immersed Samples in distilled water for various period which included 7, 14 and 21 days. Then they tested the peeling strength. It is revealed that with increased immersion time, the peeling intensity of the specimens was gradually improved in most of the cases. Authors commented that significant improvement of the peel bond strength after the water immersion suggests that water environment improve the bonding strength between the layers. This is attributed to the function of the water molecules penetrated into the composites. The penetrated water molecules are considered responsible for the increased peeling strength with increased water immersion time. The water molecules in the material would fill most or all the voids and crevices making the material more even than the original penal,

this would reduce the scatter factor during the peeling testing. Finally the water may act as a plasticizer to resist the peeling action resulting an increased peeling intensity.

Dhakal, Zhang & Richardson (2007) studied the effect of water absorption on the mechanical properties of non-woven hemp fiber reinforced unsaturated polyester (HFRUPE) composites. The tensile and flexural properties of water immersed specimens subjected aging conditions were evaluated and compared alongside dry composite specimens. As a result, the percentage of moisture uptake increased as the fiber volume fraction increased due to the high cellulose content. The tensile and flexural properties of HFRUPE specimens were found to decrease with increase in percentage moisture uptake. Moisture induced degradation of composite samples was significant at elevated temperature. The water absorption pattern of these composites at room temperature was found to follow Fickian behavior, whereas at elevated temperatures it exhibited non-Fickian. Water uptake behavior is radically altered at elevated temperatures due to significant moisture induced degradation. Exposure to moisture results in significant drops in tensile and flexural properties due to the degradation of the fiber–matrix interface.

Silva (2008) investigated a hybrid composite associating natural fibers (Curaua) and synthetic fibers (E-glass). An investigation was conducted to evaluate the degradation of the mechanical properties due to water absorption. Absorption tests were carried out and obtained the composite saturation curve for both distilled water and sea water conditions. A non-hybrid composite (just with Curaua fiber), was also evaluated for comparison. The mechanical properties were evaluated through tensile and three-point-bend tests. After the mechanical tests, author carried out a fracture characteristic analysis of the tested specimens. It is concluded that the water absorption of the laminated hybrid was higher for distilled water (2.10%) than for sea water (1.95%). However, the saturation time was approximately the same for both conditions. The more affected properties were the flexural modulus for sea water immersion and the tensile strength for distilled water immersion.

Farias, Farina, Pezzin & Silva (2009) aimed to investigate the effect of bi-dimensional orientation of leaf stalk fibers from peach palm in impact, tensile strength behavior and water absorption profile of polyester/fiber reinforced composites. They produced many varies of mentioned composites and tested with izod impact and tensile test so they obtain that notices; the composite with only weave showed moderately good water resistance compared to the composite with weave and powder. The influence of particle size in water gain percentage had distinct behavior. The micrographs of the fractured surface specimens revealed a reasonable interaction between the reinforcement and matrix.

Akil, Cheng, Mohd Ishak, Abu Bakar & Abd Rahman, (2009) studied on the effects of water absorption on mechanical properties of jute fiber reinforced with unsaturated polyester composites. They conducted water absorption tests by immersing composite specimens into three different environmental conditions included distilled water, sea water and acidic solutions at room temperature for a period up to 3 weeks. The effects of the immersion treatment on the flexural and compression characteristics were investigated. The flexural and compression properties were found to decrease with the increase in percentage water uptake. They explained these flexural and compression behaviors by the plasticization of the matrix–fiber interface and swelling of the jute fibers. They found the water absorption pattern is follow pseudo-Fickian behavior. In consequently of, exposure of the natural fiber composite materials to aqueous environments results in significantly drops in strength and modulus due to the weakening of interface between fiber and matrix. However, a significant increase in the maximum strain is observed due to the increase in ductility of natural fiber as a result of breakdown of cellulose structure after immersion process.

All the studies showed that there is a significant degradation in mechanical properties after water exposures. However, it became necessary to focus on the testing of the pipes after being exposed to natural (salty water) conditions. In particular, the dry heat and sea water exposures. In case of enough exposure duration, the material properties of FW-GFRP pipes are more severe degraded.

CHAPTER THREE
EXPERIMENTAL SETUP

3.1 Production FW-GFRP pipes

In this study, The FW-GFRP pipes were produced by a filament winding machine, Izoreel Composite Insulating Materials Ltd., Izmir, Turkey. FW-GFRP pipes were manufactured at $[\pm 55^\circ]_{3A}$ winding angles. Roving E-glass–fiber with 600 Tex and 17 μm diameter was as reinforcement. The matrix material was Epoxy Bakalite EPR 828 EL resin. The hardener material was used Epoxy Bakalite EPH 875. Mechanical properties of these matrix and reinforcement materials are given in Table 3.1. Before winding operation, resin was mixed for 4 – 5 min at 40°C resulting in an appropriate viscosity with a 4-h gel time. The fibers were wetted by passing through a resin bath for impregnation just before they were wound onto the mandrel. Helical winding was used for the desired angles of $[\pm 55^\circ]_3$. Components were cured approximately 130 ^oC along 3 hours. Afterwards; the composite tubes are cooled to room temperature. The thickness of a fiber glass/epoxy each layer was approximately 0.3 mm. The length and the inner diameter of the test specimens were 350 and 100 mm, respectively. The specimens were cut using a diamond wheel saw. Volume fraction, V_f and density of specimens were measure as 65%, 2.075 g/cm^3.

The geometry and picture of the specimen is shown in Table 3.2, Figure 3.1 and Figure 3.2, respectively.

Table 3.1 Mechanical properties of the fiber and resin

	E(GPa)	σ_{TS}(MPa)	ρ(g/cm^3)	ε_t(%)
E-glass	73	2400	2.6	4-5
Epoxy resin	3.4	50-60	1.1	6-7

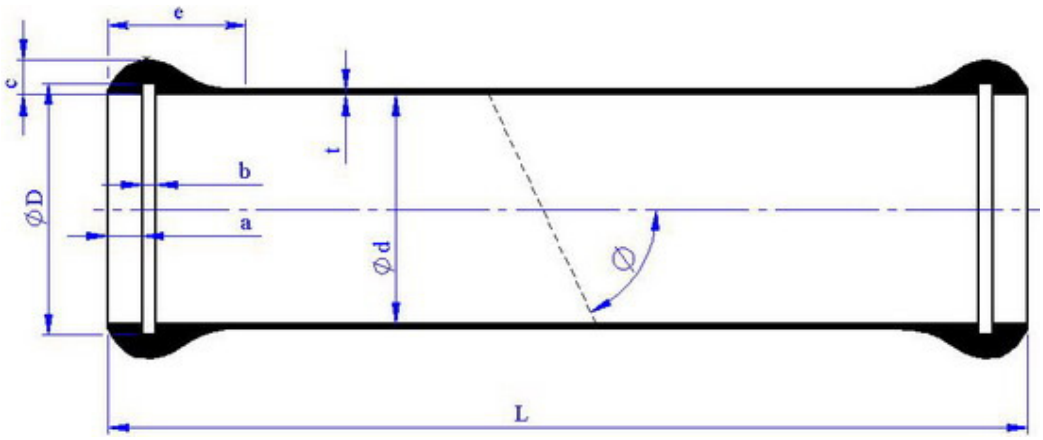

Figure 3.1 Geometry of the specimen (L= 350 mm, D= 117.6 mm, a= 20 mm, b= 6 mm, c= 15 mm, d= 100 mm, e= 60 mm, t= 1.8 mm, ϕ= 55°).

Figure 3.2 Photograph of typical test specimen.

Totally, 32 specimens (pipes) were manufactured. For experiment, distribution of specimens is given in Table 3.3. Four specimens are subjected for every impact energy values both of dry and water immersed conditions.

Table 3.3 Distribution of specimens for experiment

Impact energy / Condition	Dry Condition	Water Immersed Condition	TOTAL
Unimpacted	4*	4	8
5J	4	4	8
7.5J	4	4	8
10J	4	4	8
TOTAL	16	16	32

* Number of specimens

3.2 Sea Water Simulation

For sea water immersion tests, special barrel were fabricated. Approximately having 0.34% salinity rate, water was made with “rock salt”. 16 pipes were put into the barrel with simulated sea water (Figure 3.3).

Figure 3.3 FW-GFRP pipes under simulated sea water condition.

Every month, the specimens were taken from barrel then water was swashed by a mixing apparatus for homogeneity (Figure 3.4 and Figure 3.5).

Figure 3.4 Drill with mixer apparatus.

Figure 3.5 Application of homogenize.

After, the specimens have exposed to sea water three months; they were taken out from barrel and then subjected to impact and/or pressure tests.

3.3 Impact Testing

In this study, the impact tests are performed using Fractovis Plus impact test machine in the Composite Research Laboratory of Dokuz Eylül University to examine fracture surfaces of the tested specimens.

The Ceast-Fractovis Plus impact tester was used for low velocity impact tests for this study as shown in the Figure 3.6. Fractovis Plus test machine which was suitable for a wide variety of applications requiring low to high impact energies which generates maximum velocities up to 24 meters per second and impact energies up to 1800 Joules. The impactor, which was used to strike the pipe samples, is a hemispherical indenter nose with a 12.7 mm diameter spherical head and is connected with a force transducer with maximum loading capacity of 22.4 kN. The total impact mass including impactor nose, force transducer and crosshead was 5.02 kg. The ranges of impact energies can be obtained by choosing suitable combinations of crosshead mass and drop height of the impactor. Impactor and crosshead mass are given in Figure 3.7. The impactor was released from a chosen height and dropped

freely along the guide columns. The contact force is measured with a load transducer located on hemispherical nose. Instrumented impact test records contain the entire impact event so that the full impact force versus time profile can be analyzed. The Fractovis Plus impulse data acquisition system is the heart of impact testing system. It captures load information at very high speed from impact tests then data is analyzed graphically. The tester can get 16000 data per second from impact by request. Data acquisition system records the electronic signals and converts them into the impact parameters. The software used by the impact testing machine was capable of calculating time dependent velocity, deflection and absorbed energy values from load history given by the piezoelectric force transducer based on Newton's second law and kinematics with the assumption that the impactor is perfectly rigid.

The objective of impact testing is to determine an object's ability to resist high-rate loading, which is measured by the energy absorbed to fracture a test piece at high strain rate. Impact strength along with impact resistance is one of the most commonly measured properties and to quantify of composite structures. The impact resistance of a part is, in many applications, a critical measure of service life. More importantly these days, it involves the perplexing problem of product safety and liability (Naik, 2005).

Figure 3.6 The Caest-Fractovis Plus impact machine (and inside outlook).

Figure 3.7 Impactor and crosshead mass.

The impact characteristics, such as peak load, contact duration; maximum deflection and absorbed energy were examined against the corresponding impact energies.

The force vs. time curve can be characterized by the peak force, the energy to peak force, total energy, and displacement to maximum load. Maximum (peak) load is the highest point in the load-time curve. Often the point of maximum load corresponds to the onset of material damage or complete failure. Energy to maximum load is the energy that the sample has absorbed up to the point of maximum load. It is the area under the load/deflection curve from the test start to the maximum load point. Total energy is the energy that the sample has absorbed up to the end of the test, when the load reaches zero again. It is the area under the load/deflection curve from the test start to the test end. Deflection to maximum load is the distance the impactor traveled from the point of impact to the point of maximum load (Naik, 2005).

Here the peak load is the maximum contact force between the impactor and the composite tube at the contact point. Contact duration is determined as the total time of contact between the impactor and the composite tubes. The maximum deflection of a composite tube is defined as the largest depth on the top surface from the initial position. The absorbed energy is the energy consumed between the impactor and the specimen through the formation of damage and friction.

Impact load as a function of time f(t) and projectile tip displacement as a function of time x(t) given by relation (3.1) and (3.2) respectively.

$$f(t) = m_o a(t) \tag{3.1}$$

$$x(t) = \int \left(v_o + \int a(t)dt \right) dt \tag{3.2}$$

where; a(t): Acceleration, $m_{o:}$ Projectile mass, v_o: Projectile velocity just before impact.

3.3.1 Design of V-block

A V-block apparatus for the impact testing of the tube was designed. The V-block holder has a 90° included angle. It is fabricated using steel. The side supports is of sufficient depth to support the specimen in the V and not on the top edges of the V-block. The specimen's tubes rests on a V-block test fixture with rigidly fixed to the tower frame as shown in Figure 3.8

Figure 3.8 V-block test fixture and specimen for impact.

The first step in testing was determining of the impact energy loads. So, some specimens (out of 32 original specimens) were tested under varied impact energies from 5J to 25J. Because if impact energy does not result in damage, in fatigue test, fatigue life will be infinite or if impact cause larger damage areas, fatigue live (fatigue cycles) will be small as much as not to compare with each other or not to observe impact effect. In addition in static test, wrong chosen impact energy can be faced us with results which more closed each other caused wrong estimations.

Once the appropriate energy levels were determined, the impacts were performed at three different energy levels as 5J, 7.5J, and 10J using an impact test machine at

temperatures of 25 °C (at room condition). After then impacted and non-impacted specimens were subjected to fatigue loading.

3.4 Fatigue Testing

Internal dynamic (fatigue) pressure testing method was applied to the composite tubes in close-ended condition by PLC controlled servo-hydraulic testing machine. The procedure for determining burst pressure and fatigue life of composite pressure vessels is based on some standards. Test specimens were loaded with internal pressure using a 1 MPa/min loading rate up to burst pressure. Test machine has range of 0-250 bars. It could test two pipes at the same time. For dynamic loading conditions, the fatigue tests are performed maximum at 0.5 Hz frequency. There are four type emergency stop on machine for safety and productivity. Test machine is shown Figure 3.9.

Figure 3.9 PLC controlled servo-hydraulic testing machine.

3.4.1 Experimental Setup

During all the internal pressure tests, following test apparatus was used to satisfy the closed-end conditions of the composite tubes. The test apparatus and its equipments are convenient to create the closed-end condition to ensure the generalized plane strain case. Photographs of test apparatus and their set-up state in Figure 3.10 and Figure 3.11, respectively. Sectional and general cutaway views of a part of prepared specimen are given in Figure 3.12 and Figure 3.13 respectively.

Figure 3.10 A photograph of test apparatus.

Figure 3.11 A photograph of set up state of test apparatus.

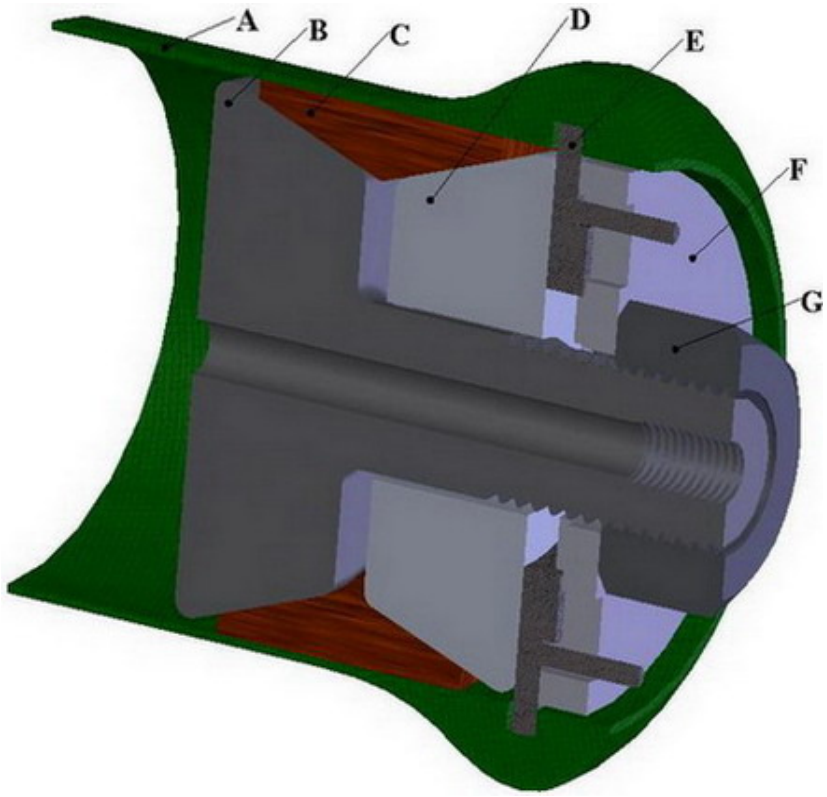

Figure 3.12 Cutaway view of a part of prepared specimen for internal pressure testing and subsections (Onder, 2009). A: Composite pressure vessel; B, D : Compressing parts; C : Rubber seal element ;E : System locking member component; F : Flange; G : Nut.

Figure 3.13 Cutaway view of prepared specimen for internal pressure testing (Onder, 2009).

A protective test box was manufactured for observing the test specimen during pressure tests. It protects the harmful effects of the hydraulic oil during bursting of the specimens as seen in Figure. It provides the observers' protection from the test specimen while taking photos and videos. Figure 3.14 shows a photo of the protective test box.

Figure 3.14 A protective test box.

After impacted and unimpacted specimens were prepared, to first failure and burst failure pressures of pipes were measured. In the dynamic loading, inner pressure was performed from 30% to 70% of burst strength of the pipe. Burst pressures were found from average values of the tests results, given information about correlation between impact induced damages and burst pressures.

CHAPTER FOUR
RESULTS AND DISCUSSIONS

4.1 Impact testing

In this study, 24 tests were performed under impact energies as 5J, 7.5J, and 10J in order to examine damage process in stacking sequences $[\pm 55°]_3$ at room temperature. It is known that in composite tubes impacted with low energy, degradation will be localized in the composite tube wall in the area closest to the contact point. Inspection of fractured pieces was done after each test. First damage created with 5J impact energies involves small delaminations, relatively. At higher energies these delaminations propagate and are accompanied by the multiple intralaminar delaminations. Images of impacted pipes are given in Figure 4.1. It is clearly seen that delamination (damage area) is increased with increasing impact energy.

The impact characteristics such as peak force, maximum deflection and total absorbed energy are listed against the corresponding impact energies in Table 4.1, 4.2. These parameters are very important for FW-GFRP pipes subjected to impact loading. Also, Impact test results of composite pipes for both dry and water immersed conditions are given in Figure 4.2, 4.3 and 4.4.

It is clearly seen that peak force, maximum deflection and total absorbed energy are increased with impact energy. The peak force values of water immersed specimens seem to be greater than dry specimens. In addition max deflection and total absorbed energy values have antipodal. This is likely due to that, pipes behave plastically and becomes more flexible as exposed to sea water.

(a) **(b)** **(c)**

Figure 4.1 Illustration of impacted surface for three corresponding energy levels of the composite tubes (a) 5J, (b) 7.5J, and (c) 10J.

Table 4.1 Impact Properties of FW-GFRP composite pipes for dry condition

SPECIMENS (Dry condition)	Peak Force (N)	Maximum Deflection (mm)	Total Absorbed Energy (J)
5J1	1269.29	6.1384	4.13
5J2	1266.77	6.4306	4.34
5J3	1288.82	6.1466	4.18
5J4	1237.16	6.3603	4.28
5J average	1265.51	6.27	4.23
7.5J1	1561.57	7.5478	6.05
7.5J2	1457.00	8.5134	6.30
7.5J3	1512.44	7.5303	6.06
7.5J4	1532.28	8.0299	5.90
7.5J average	1515.82	7.91	6.08
10J1	1615.43	9.8139	9.32
10J2	1721.57	9.5734	8.37
10J3	1705.82	9.6577	8.57
10J4	1752.44	9.4606	8.37
10J average	1698.81	9.63	8.66

Table 4.2 Impact Properties of FW-GFRP composite pipes for sea water immersed condition

SPECIMENS (Immersed condition)	Peak Force (N)	Maximum Deflection (mm)	Total Absorbed Energy (J)
5J1	1433.70	7.0504	2.92
5J2	1245.67	6.0767	3.58
5J3	1427.71	5.7552	3.03
5J4	1346.77	5.818	3.42
5J average	1363.46	6.18	3.24
7.5J1	1661.73	6.512	4.80
7.5J2	1663.93	6.4076	4.54
7.5J3	1571.02	7.012	4.50
7.5J4	1570.70	7.126	3.55
7.5J average	1616.85	6.76	4.35
10J1	1834.96	8.9675	6.99
10J2	1775.43	9.102	7.26
10J3	1782.67	9.002	7.67
10J4	1823.62	9.1486	6.91
10J average	1804.17	9.06	7.21

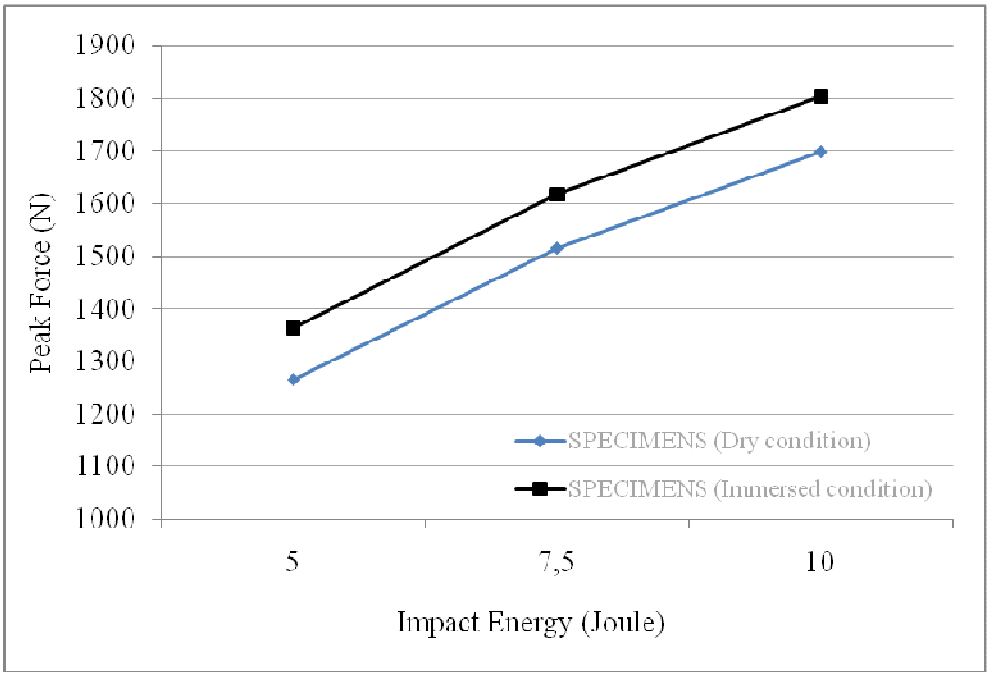

Figure 4.2 Peak force to impact energy graphs of the specimens in dry and immersed condition.

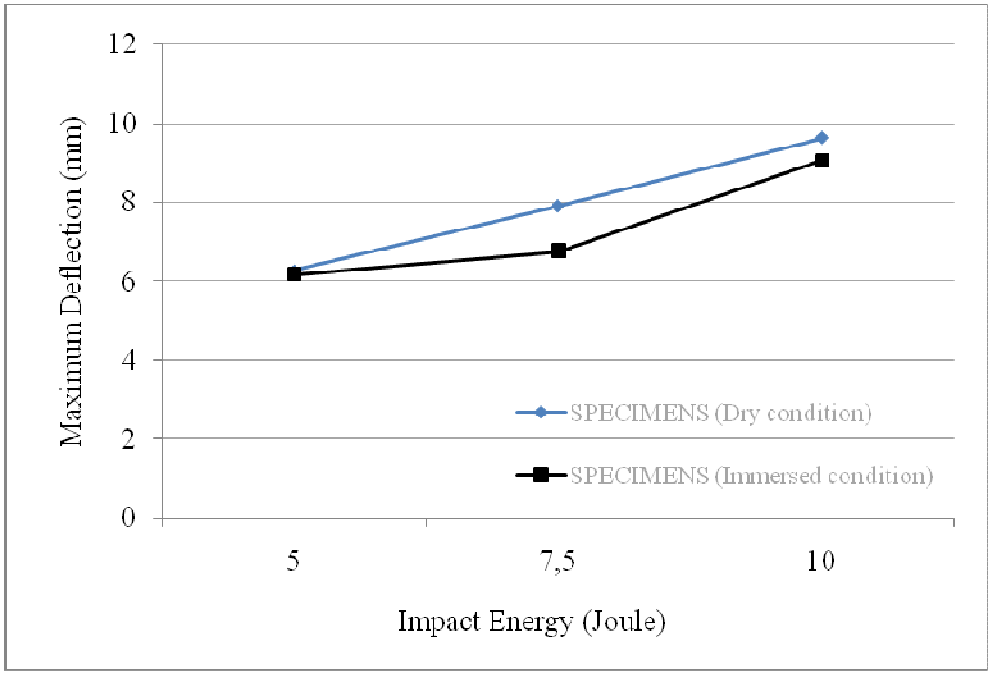

Figure 4.3 Maximum deflection to impact energy graphs of the specimens in dry and immersed condition.

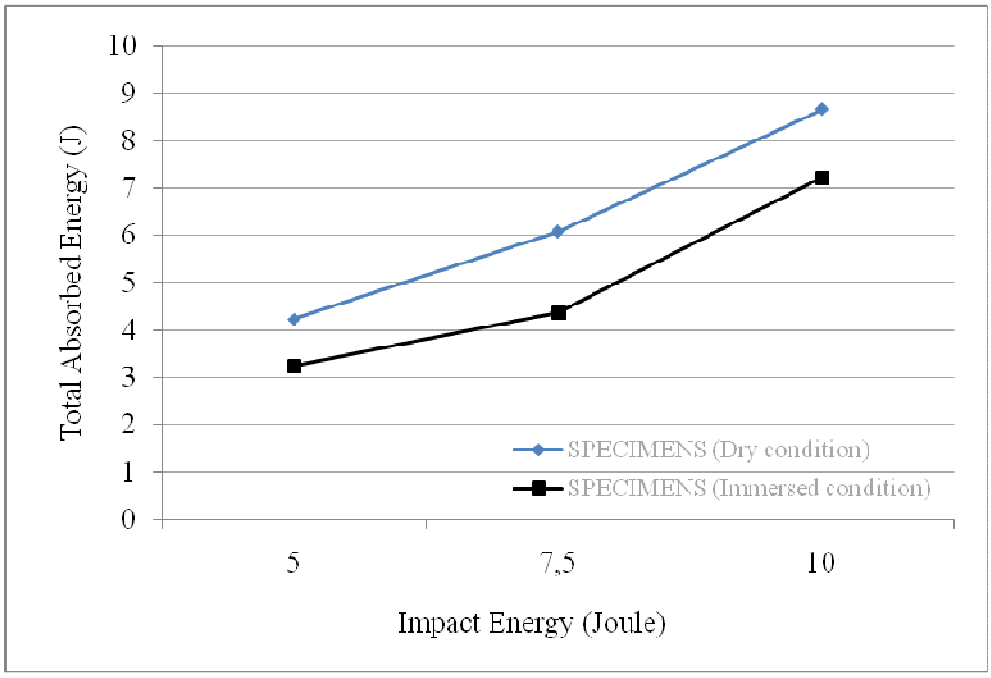

Figure 4.4 Total absorbed energy to impact energy graphs of the specimens in dry and immersed condition.

The load–deflection curves give significant opinion about the impact response of composite materials tested. Characteristic of load-deflection curves also includes some useful tips in assessing damage process of composite tubes. Absorbed energy in an impact event can be calculated from load-deflection curves.

Load-deflection curves, in general, can be classified as; closed type curve. As long as a closed curve is observed it is possible to say that the impact loading does not result in a serious damage to the specimen. The rebounding case results in closed curves indicating the rebounding of the impactor from the specimen surface. The load–deflection curve turned toward the origin of the diagram after reaching a maximum force (rebounding).

In this study, typical load-deflection curves of the composite pipes subjected to impact loading have one situation, rebounding. These curves are seen for 5J, 7.5J, and 10J in Fig. 4.5 to 4.9. Peak force is increased with increasing performed impact

energy. Likewise the maximum deflection values increase with increasing impact energy.

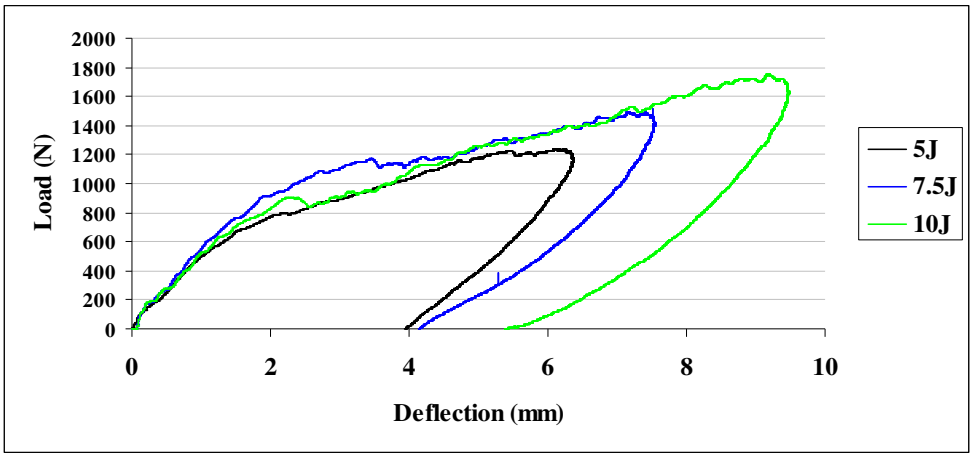

Figure 4.5 Comparison of 5J, 7.5J and 10J impacts Load- Deflection curves for dry condition.

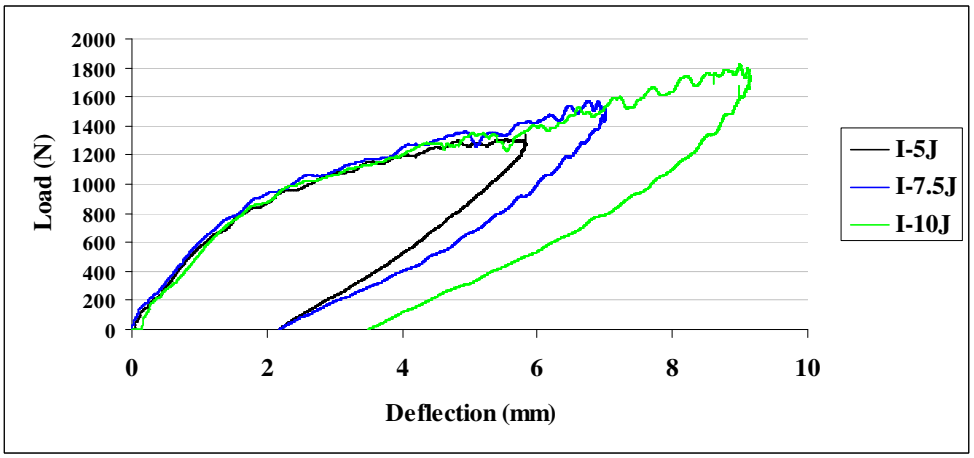

Figure 4.6 Comparison of 5J, 7.5J and 10J impacts Load- Deflection curves for immersed condition.

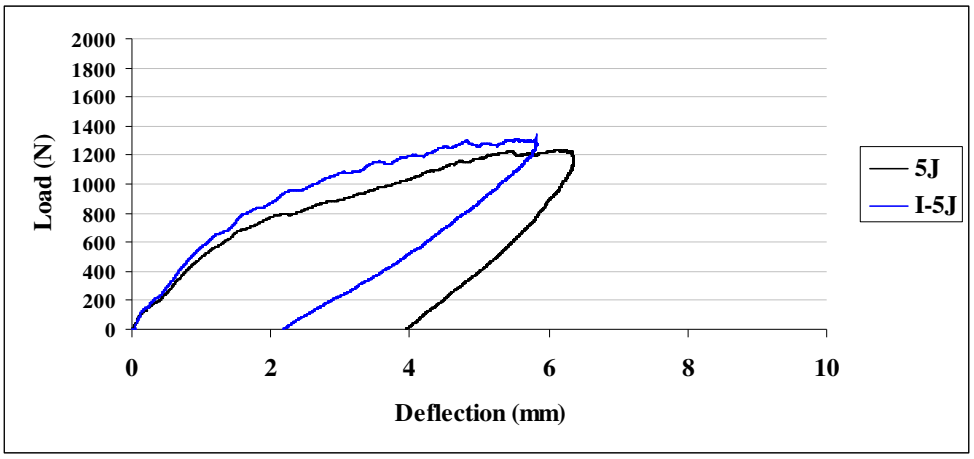

Figure 4.7 Comparison of condition type of Load- Deflection curves for 5J impact.

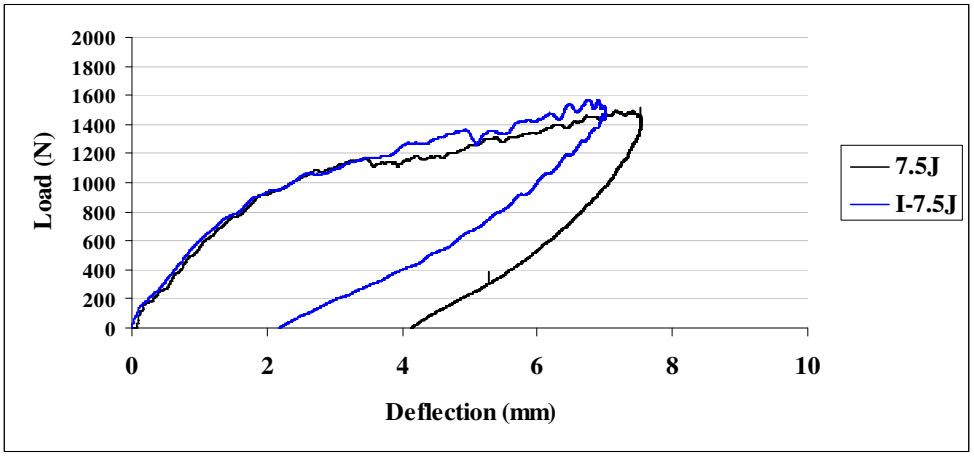

Figure 4.8 Comparison of condition type of Load- Deflection curves for 7.5J impact.

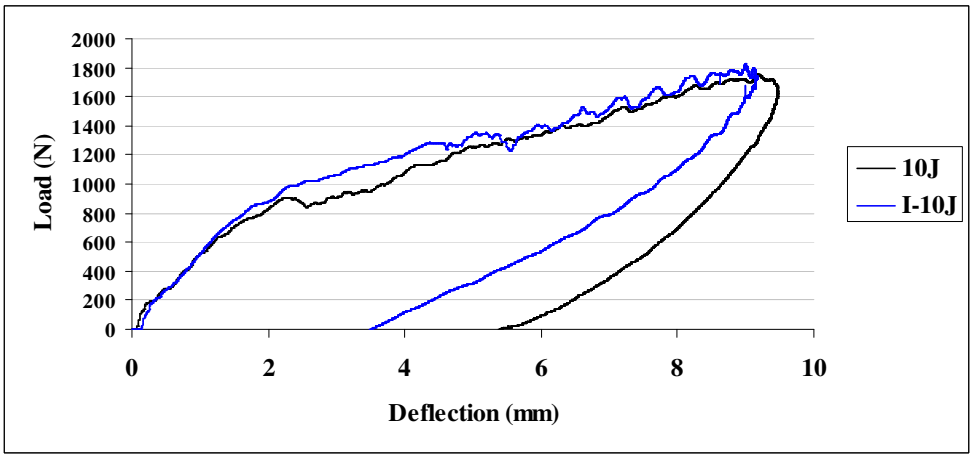

Figure 4.9 Comparison of condition type of Load- Deflection curves for 10J impact.

Load-Time curves were generated for impact tests and it is given in Figure 4.10 to 4.14. As can be seen from these figures the maximum time values increase with increasing impact energy. Also the average position of each curve gives us a hint about the impact sensitivity of tubes.

It is seen in all graphs immersed specimens have little more contact duration and peak force than dry specimens.

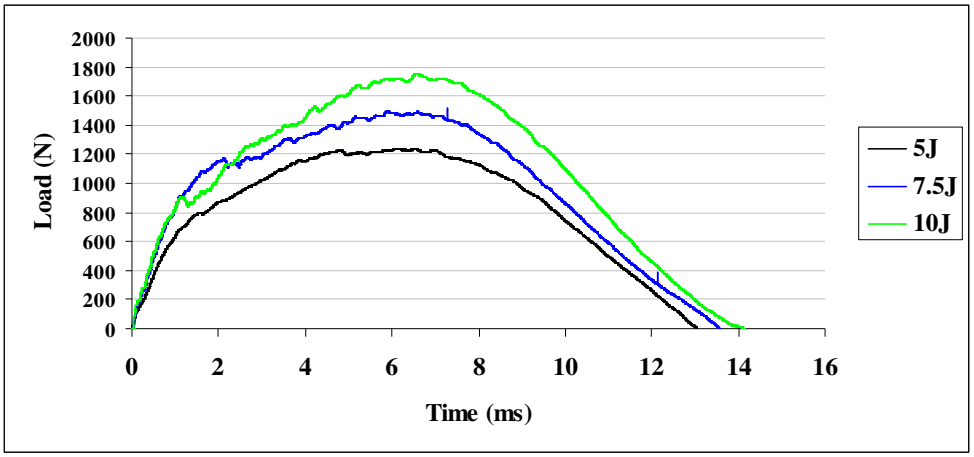

Figure 4.10 Comparison of 5J, 7.5J and 10J impacts Load- Time curves for dry condition.

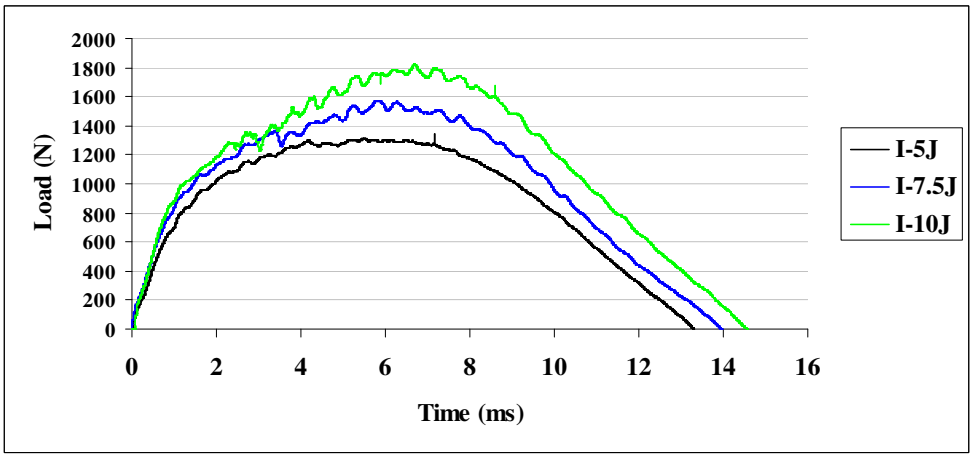

Figure 4.11 Comparison of 5J, 7.5J and 10J impacts Load- Time curves for immersed condition.

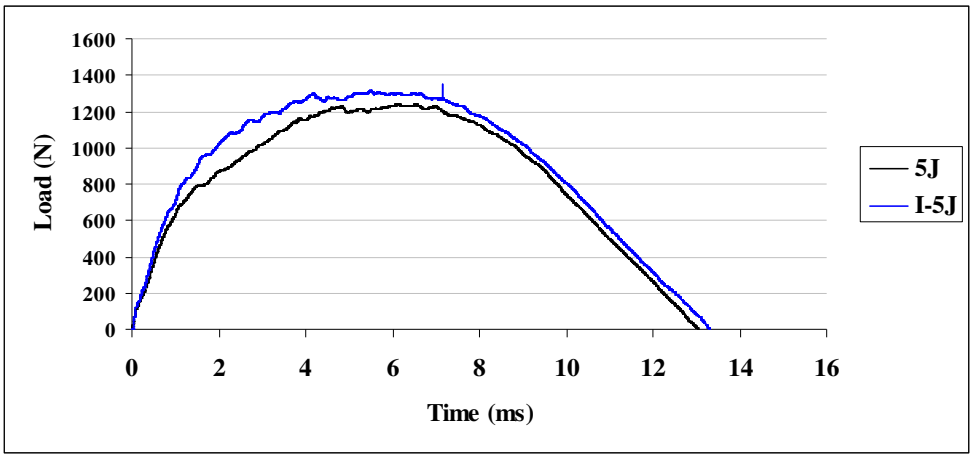

Figure 4.12 Comparison of condition type of Load-Time curves for 5J impact.

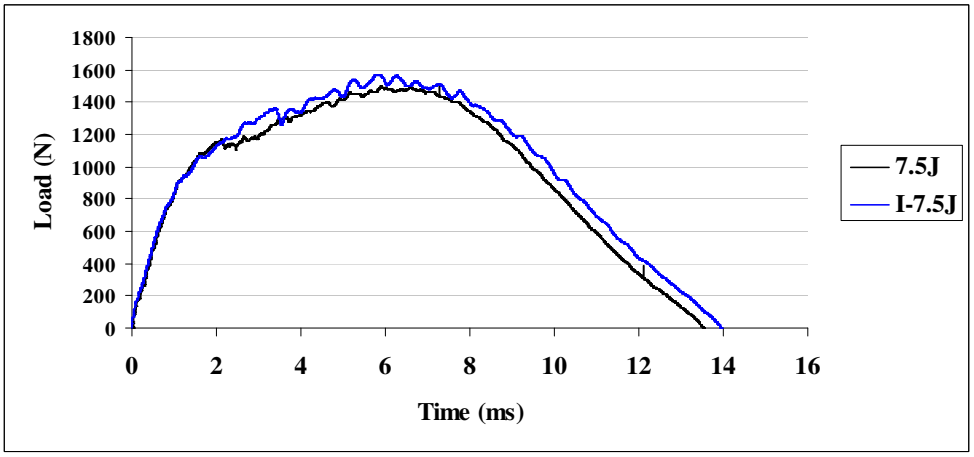

Figure 4.13 Comparison of condition type of Load-Time curves for 7.5J impact.

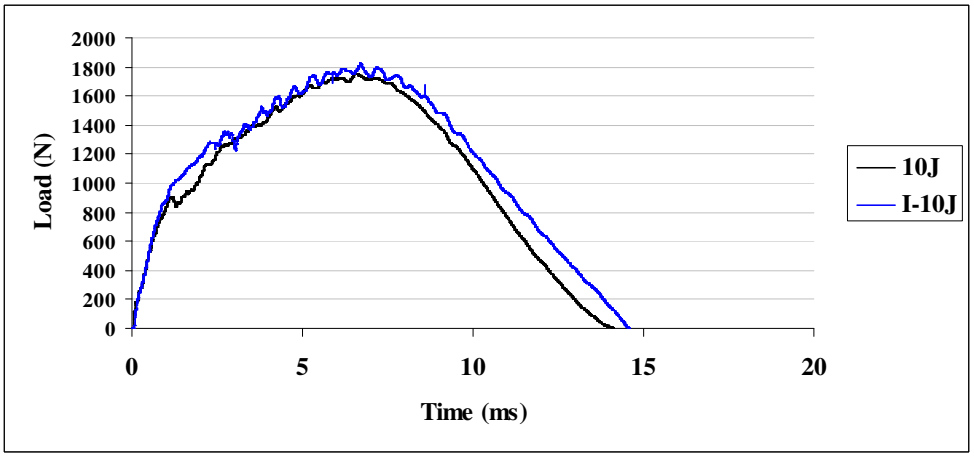

Figure 4.14 Comparison of condition type of Load-Time curves for 10J impact.

4.2 Fatigue Testing

In the tests, the average static burst pressure values of the weakest specimens (subjected 10J impact) were calculated experimentally. Subsequently, dynamic (fatigue) tests were applied in 20% and 70% scale of mentioned burst pressure value. This value is observed approximately 60 bars so that selected ranges of fatigue loading were 12 to 42 bars. The low cycle tests were applied with 0.5 Hz frequency and cycle type was selected punch type.

For fatigue tests, 32 tests are aimed to realize that they are given in Table 4.3.

Table 4.3 Distribution of specimens for experiment

Impact energy / Condition	Dry Condition	Water Immersed Condition	TOTAL
Unimpacted	4*	4	4
5J	4	4	4
7.5J	4	4	4
10J	4	4	4
TOTAL	16	16	32

* Number of specimens

After impact, they lose their load carrying ability and the buckled region becomes the weakest link when fibers buckling. Failure will initiate from this region from the subsequent pressure loading. For impacted tubes, the failures have initiated from the impact location. The failure cases of unimpacted specimens are different from impacted. It was apparent that the failure origins of the unimpacted tubes were initiated away from the middle location of the tube was totally unexpected. Figure 4.15 shows tubes subjected to 0J impact energy leaked on corner of the tube; subjected 7.5J impact specimen leaked on around of impact location; finally subjected 7.5J impact specimen leaked on impact location, respectively.

During the fatigue testing three damage mechanism stages were observed. The first damage mechanism is perspiration. Matrix cracking started at the inner surface of the tubes then matrix crack's size increased. The perspiration begins at the center of impacted are region as a small oil droplet. Latter stage is a leakage that leakage

initiates when the matrix cracks coalescence reached the point in which the pressurized oil can penetrate through these cracks to reach the surface of the tube as surface wetting. Due to cracks coalescence from inner surface towards outer surface, a leakage path is formed. After a few cycles, the tubes reach the point where small matrix cracks turn into bigger cracks that allow an intense oil leakage. At each cycle, the oil penetrates through the matrix cracks and helps to open them, and the cracks coalesce quickly and turn the slight leakage into intense leakage. So, it is observed that these cracks have opened and closed at each cycles by means of internal pressure. Leakage increased gradually with continuing of cycling. After then with damage propagation, on the specimens, jet case is occurred. The composite tubes were loaded internal pressure until failure. Therefore, in tests after a few numbers of cycles (about 2000-3000) the test is finished. Phases of fatigue life of specimen are demonstrated in Figure 4.16 to 4.24. Perspiration phases are not demonstrated on figures due to needing camera with too much high solution to observe oil droplet.

(a) **(b)** **(c)**

Figure 4.15 Illustration of fatigued specimens for three corresponding type of the leakages (a) 10J, (b) 7.5J and (c) 7.5J

Figure 4.16 Leakage state of fatigue loading of composite pipe.

Figure 4.17 Advanced leakage state of fatigue loading of composite pipe.

Figure 4.18 Strong leakage state of fatigue loading of composite pipe.

Figure 4.19 Jet I state of fatigue loading of composite pipe.

Figure 4.20 Jet II state of fatigue loading of composite pipe.

Figure 4.21 Jet III state of fatigue loading of composite pipe.

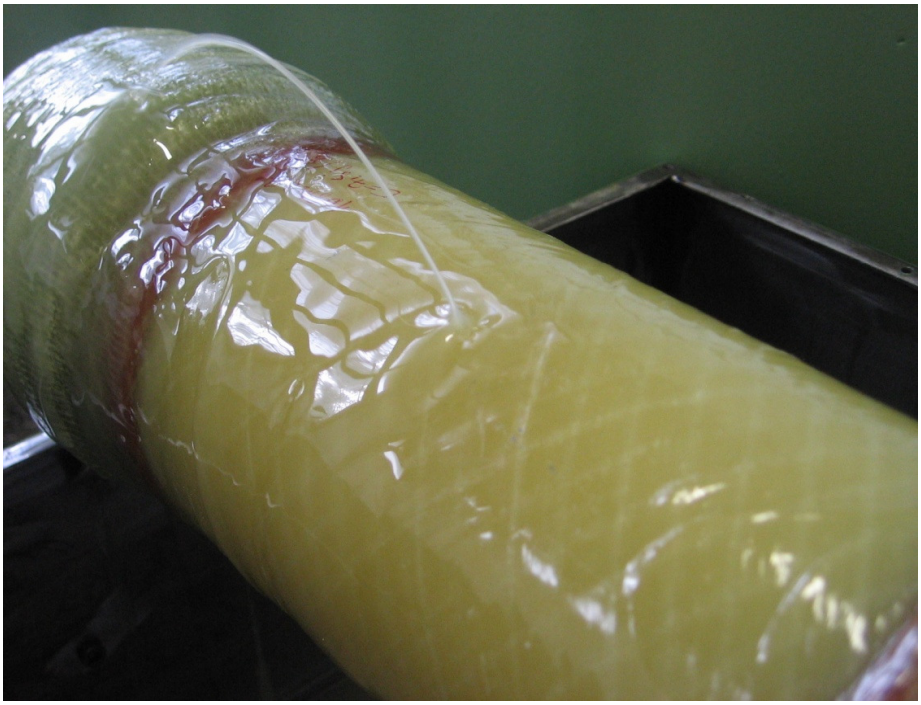

Figure 4.22 Jet IV state of fatigue loading of composite pipe.

Figure 4.23 Exact jet state of fatigue loading of composite pipe.

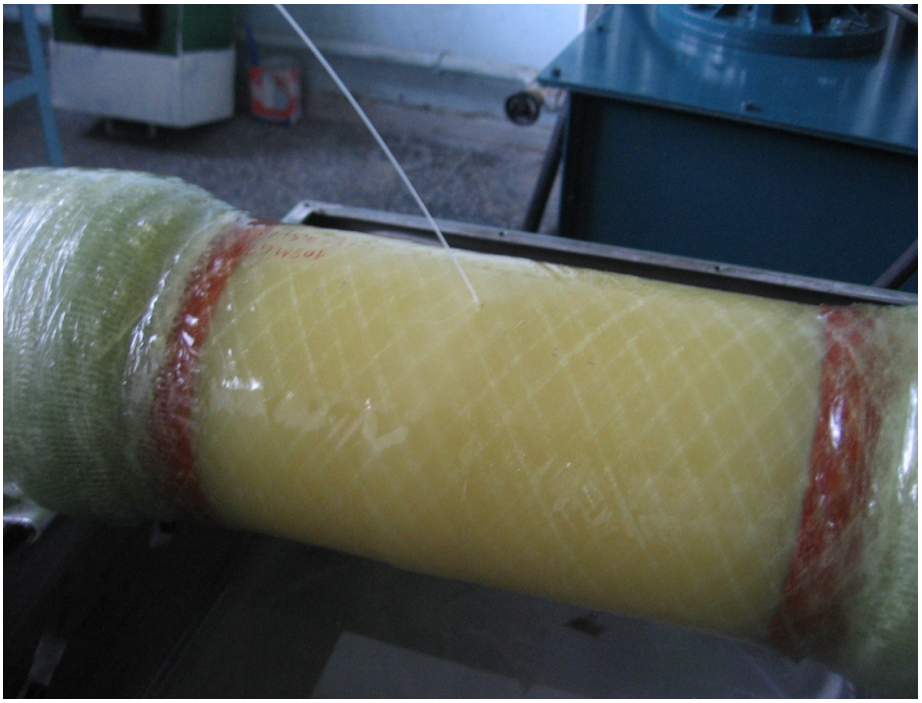

Figure 4.24 Eruption state of fatigue loading of composite pipe.

In order to determine the fatigue life, “the perspiration state” is selected for utilization of the performance limit of the pipes.

In Table 4.4, perspiration and leakage failure cycles of water immersed and dry condition specimens are given.

Table 4.4 Average cycle number for corresponding impact energy on dynamic test of composite tubes

Specimens For Dynamic Loading	Dry condition		3rd month immersed	
	Perspiration Failure Cycles	Leakage Failure Cycles	Perspiration Failure Cycles	Leakage Failure Cycles
0J-1	47300	81447	60000	-
0J-2	17369	24200	-	-
0J-3	-	-	-	-
0J-4	51111	-	41000	60000
0J- Average	38593	52824	50500	60000
5J-1	36	1800	16250	27500
5J-2	2952	3600	19750	32500
5J-3	2354	8000	-	-
5J-4	10287	17147	-	-
5J- Average	3907	7637	18000	30000
7.5J-1	-	4532	-	29145
7.5J-2	30	1200	20000	21727
7.5J-3	30	-	11639	14014
7.5J-4	1805	2100	6373	-
7.5J- Average	622	2611	12671	21629
10J-1	-	73	-	8500
10J-2	-	29	-	800
10J-3	-	575	3500	15089
10J-4	-	610	-	-
10J- Average	161	322	3500	8130

Average fatigue cycle to impact energy curve graphs are given below in Figure 4.33. Figure 4.34 are derived from above Table 4.4.

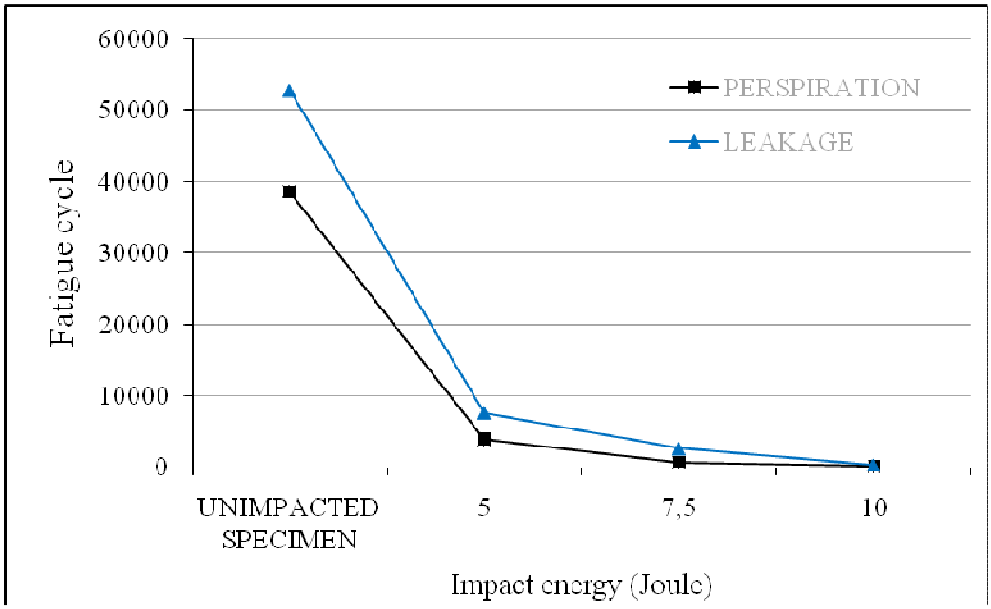

Figure 4.33 Average cycle-impact energy curve for dry condition.

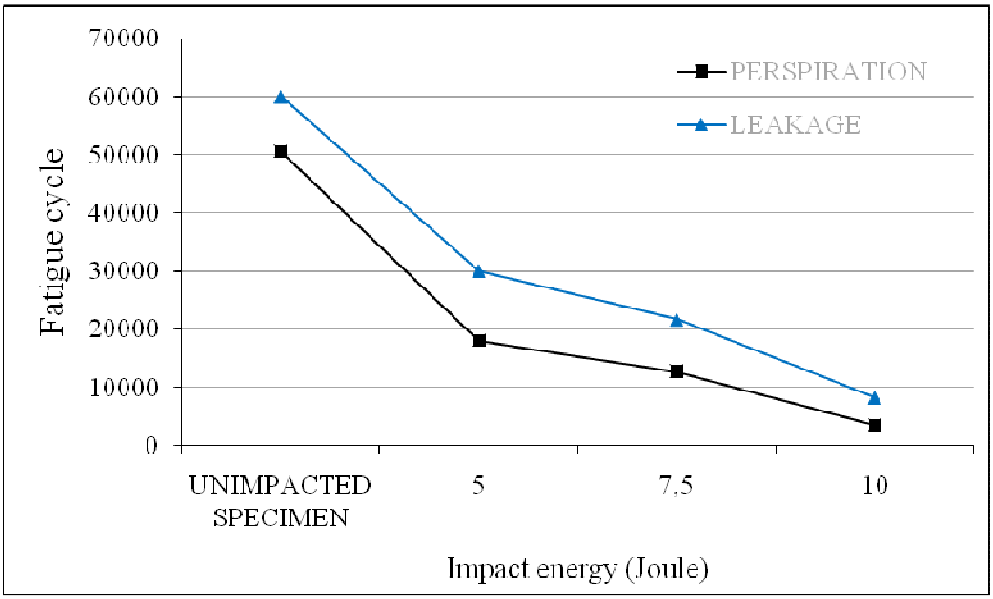

Figure 4.34 Average cycle-impact energy curve for sea water immersed condition.

The graphs show that the fatigue life cycles decrease with increasing impact energy. It can be clearly observed that the designs performed at 10J impact shows the lowest fatigue cycles values.

4.2.1 Fatigue Observations

In general, about tests specimens within dry condition can be comment like below.

In total 16 experiments, result of completion dynamic loading, one of the specimens (0J-3) had no damage (perspiration, leakage or eruption). Four of the specimens are shown regression and unstable leakage. Also It is seen that leakage on 8 specimens and jet on 6 specimens.

For unimpacted specimens, the owing to too much cycles than impacted specimens some tests have being continued 30-40 hours. In general, the perspiration is considered as first failure point. Since the damage propagation required too much cycles, advanced leakage and jet phases are not seen.

On second and third specimens of subjected to 5J impact energy, regressions are seen. With the experiment that has too much cycle and more specimens, estimations will be closer to the absolute truth. Consequently, in some specimens progressive fatigue mechanic has not been seen as estimated.

Results' dynamic loading of 7.5J and 10J impacted specimens have carried out as estimated so leakage and jet developed with gradually are understood for trend of cycle numbers.

In general, about tests specimens within sea water immersed condition can be comment like this. In total 16 experiments, result of completion dynamic loading, five of the specimens (0J-2, 0J-3, 5J-3, 5J-4 and 10J-4) have not carried out because of they had no damage (perspiration, leakage or eruption). Other tests of water immersed condition have displayed same trend like dry condition. One disparity most of failure phase have higher cycle than dry condition specimens.

CHAPTER FIVE
CONCLUSIONS AND RECOMMENDATIONS

5.1 Conclusions

This section presents the conclusions obtained from the analysis of the experimental data of low velocity impact and fatigue tests conducted on the filament wound-glass fiber reinforced plastic (FW-GFRP) pipes. Also the sea water effect on the fatigue life is studied. The following results are noticed from study;

5.1.1 Results of the Impact Tests

- Firstly, the transverse impact behaviors of the FW-GFRP pipes are examined.
- The impact characteristics, such as peak load, contact duration, maximum deflection vs. impact energies are plotted.
- Load-deflection curves of all impact tests have one case, rebounding. So none of specimens are perforated.
- First damage created under 5J, caused small delaminations including matrix and fiber cracking. At higher energies these delaminations propagate and are accompanied by the delaminations.
- It is clearly seen that contact time, peak force, maximum deflection and total absorbed energy are increased due to increasing impact energy both of the type of specimen, for all that the peak force values of water immersed specimens have trended greater than dry specimens in addition max deflection and total absorbed energy values have antipodal. Because of mentioned state is estimated as sea water immersion has become more plasticize to pipes so that pipes are behaved more flexible.

5.1.2 Results of the Fatigue Tests

- For unimpacted tubes, the failures that initiated away from the middle location of the tube were totally unexpected. On the other hand, naturally, the failure of the impacted tubes was initiated from the impact area.

- Three damage mechanism stages were observed perspiration, leakage and jet failure.
- For every failure states, impact energy-cycle curves obtained from fatigue tests.
- In order to determine the fatigue life, the perspiration stage is considered to determine load carrying capacity of tubes.
- Some of the specimens have shown regression and unstable leakage during tests.
- The graphs show that the fatigue life decrease rapidly (like a parabolic) with increasing impact energy.

5.1.3 Results of the Sea Water Effect

- After definite time (term), water (H_2O) immersion has damaged bonds of polymer which provided interlaminar connection. It is seen that 3 months weren't enough for mentioned stage.
- It the increase in the impact strength and fatigue strength of the FW-GFRP pipe is due to plasticization of the matrix by the absorbed water.

5.2 Recommendations

Following are some of the recommendations for any future work to be carried out on FW-GFRP pipes and effect of environmental conditions to FW structures;

- Voids within the composites are affected negatively on material properties. Production of these pipes including the void effects should be considered. Hence, improvement of FW-GFRP pipes production processes may contribute to consistent results in future.
- Carrying out of fatigue tests takes long time, in addition mounting and de-mounting of test apparatus have necessitated very high sleight and time so that development of test apparatus very important for productivity of fatigue tests.
- Fatigue test consist from hybrid (manual and electronic) system, controlling are required regularly by human. The test system can be improved fully automatic

- computer-controlled and joined acoustic emission system for sensitive observing.
- Microscopic analysis of the impact damaged specimens can be carried out to have an in-depth failure analysis.
- Test specimens must are exposed the sea water immersion 6, 9 and 12 months too, for seeing further damage mechanism of it.

REFERENCES

Abrate, S. (1998). *Impact on composite structures*. Cambridge: Cambridge University Press.

Akil, H. M., Cheng, L. W., Mohd Ishak, Z. A., Abu Bakar, A., & Abd Rahman, M. A. (2009). Water absorption study on pultruded jute fiber reinforced unsaturated polyester composites. *Composites Science and Technology*, 69, 1942–1948.

Arikan, H. (2010). Failure analysis of [±55°] filament wound composite pipes with an inclined surface crack under static internal pressure. *Compos ite Structures*, 92, 182–187.

Atas, C. (2004). *Large deformations in composite laminated plates. Doctor of Philosophy thesis*. Izmir: Faculty of School Natural and Applied Sciences of Dokuz Eylul University.

Avci, A., Sahin, O. S., & Tarakcioglu, N. (2007). Fatigue behavior of surface cracked filament wound pipes with high tangential strength in corrosive environment. *Composites*, Part A, 38, 1192–1199.

Bie, H., Li, X., Liu, P., Liu Y., & Xu, P. (2009). Fatigue life evaluation of high pressure hydrogen storage vessel. *International Journal of Hydrogen Energy*, in press.

Chang, D. J. (2003). Burst tests of filament-wound graphite-epoxy pipes. *Journal of Composite Materials*, 37, 811-829.

Chang, R. R. (2000). Experimental and theoretical analyses of first-ply failure of laminated composite pressure vessels. *Composite Structures*, 49, 237-243.

Changliang Z., Mingfa R., Wei Z., & Haoran C. (2006). Delamination prediction of composite filament wound vessel with metal liner under low velocity impact. *Composite Structures,* in press.

Chib, A. (2003). *Parametric study of low velocity impact analysis on composite tubes*. Master of Science thesis. Maharashtra: Faculty of School Natural and Applied Sciences of Wichita State University.

Curtis, J., Hinton, M. J., Li, S., Reid, S. R., & Soden, P. D. (2000). Damage, deformation and residual burst strength of filament-wound composite pipes subjected to impact or quasi-static indentation. *Composites*, Part B, 31, 419-433.

Davies, P., Mazeas, F., & Casari, P. (2001). Sea water aging of glass reinforced composites: shear behavior and damage modelling. *Journal of Composite Materials*, 35, 1343–30.

Davies, P., Riou, L., Mazeas, F., & Warnier, P. (2005). Thermoplastic composite cylinders for underwater applications. *Journal of Thermoplastic Composite Materials*, 18 (5), 417-443.

Dhakal, H. N., Zhang, Z. Y., & Richardson, M. O. W. (2007). Effect of water absorption on the mechanical properties of hemp fiber reinforced unsaturated polyester composites. *Composites Science and Technology*, 67, 1674–1683.

Dogan, T. (2006). *Prediction of composite vessels under various loadings. Master of Science thesis*. Izmir: Faculty of School Natural and Applied Sciences of Dokuz Eylul University.

Doyum, A. B., & Altay, U. B. (1997). Low-velocity impact damage in glass fiber/epoxy cylindrical tubes. *Materials & Design*, 18 (3), 131–135.

Erkal, S. (2007). *Fatigue damage on composite cylinders. Master of Science thesis.* Izmir: Faculty of School Natural and Applied Sciences of Dokuz Eylul University.

Farias, M. A., Farina, M. Z., Pezzin, A. P. T., & Silva, D. A. K. (2009). Unsaturated polyester composites reinforced with fiber and powder of peach palm: Mechanical characterization and water absorption profile. *Materials Science and Engineering*, C 29, 510–513.

Filament winding, (n.d.). Retrieved May 1, 2010, from http://en.wikipedia.org/wiki/Filament_winding

Filament wound materials, (n.d.). Retrieved May 1, 2010, from http://www.ckcomposites.com/technical-data.php

Gellert, E. P., & Turley, D. M. (1999). Sea water immersion ageing of glass-fiber reinforced polymer laminates for marine applications. *Composites*, Part A, 30, 1259–1265.

Gemi, L., Tarakcioglu, N., Akdemir, A., & Sahin, O. S. (2009). Progressive fatigue failure behavior of glass/epoxy $[\pm 75^\circ]_2$ filament-wound pipes under pure internal pressure. *Materials and Design*, 30, 4293–4298.

Gning, P. B., Tarfaoui, M., Collombet, F., & Davies, P. (2005). Prediction of damage in composite cylinders after impact. *Journal of Composite Materials*, 39 (10), 917–928.

Gning, P. B., Tarfaoui, M., Collombet, F., Riou, L., & Davies, P. (2005). Damage development in thick composite pipes under internal loading and influence on implosion pressure: experimental observations. *Composites*, Part B, 36, 306-318.

Gu, H., & Hongxia, S. (2007). Effect of water absorption on the mechanical properties of glass/polyester composites. *Materials and Design*, 28, 1647–1650.

Gu, H., & Hongxia, S. (2008). Delamination behavior of glass/polyester composites after water absorption. *Materials and Design*, 29, 262–264.

Jones R. M. (1999). *Mechanics of composite materials*. (2nd ed.). Philadelphia: Taylor & Francis Group LLC.

Kaneko, T., Ujihashi, S., Yomoda, H., & İnagi, S. (2008). Finite element method failure analysis of a pressurized FRP cylinder under transverse impact loading. *Thin Walled Structures*, 46, 898–904.

Karbhari, V. M., Haller, J. E., Falzon, P. K., & Hersberg, I. (1999). Post-impact crush of hybrid braided composite tubes. *International Journal of Impact Engineering*, 22, 419-433.

Kelkar, A. D., Jitendra, S., Bolick, T., & Bolick, R. (2003). Introduction to low cost manufacturing of composite laminates. *Proceedings of the 2003 American Society for Engineering Education Annual conference & Exposition*, Session 2003-1482.

Khalid, Y. A., Hamed, A. F., & Sapuan, S. M. (2007). Pressure carrying capacity of reinforced plastic tubes. *Polymer-Plastics Technology and Engineering*, 46, 651–659.

Kim, U. C., Kang, J. H., Hong C. S., & Kim C. G. (2005). Optimal design of filament wound structures under internal pressure based on the semi-geodesic path algorithm. *Composite Structures*, 67, 443–452.

Kobayashi, S., İmai, T., & Wakayama, S. (2007). Burst strength evaluation of the FW-CFRP hybrid composite pipes considering plastic deformation of the liner. *Composites*, Part A, 38, 1344–1353.

Kootsookos, A., & Mouritz, A. P. (2004). Sea water durability of glass- and carbon-polymer composites. *Composites Science and Technology*, 64, 1503–1511.

Liao, K., Schulthelsz, C. R., & Hunston D. L. (1999). Effects of environmental aging on the properties of pultruded GFRP. *Composites*, Part B, 30, 485–493.

Mallick, P.K. (2007). *Fiber-reinforced composites : materials, manufacturing, and design*. (3rd ed.). Boca Raton: Taylor & Francis Group, LLC.

Mazumdar, S. K. (2002). *Composites manufacturing : materials, product, and process engineering*. Boca Raton: CRC Press LLC.

Naik, M. K. (2005). *The effect of environmental conditions on the hydrostatic burst pressure and impact performance of glass fiber reinforced thermoset pipes*. Master of Sicience thesis, Dhahran: Faculty of School Natural and Applied Sciences of Kinh Fahd University of Petroleum & Minerals.

Onder, A. (2007). *First failure pressure of composite pressure vessels. Master of Science thesis*. Izmir: Faculty of School Natural and Applied Sciences of Dokuz Eylul University.

Onder, A., Sayman, O., Dogan, T., & Tarakcioglu, N. (2009). Burst failure load of composite pressure vessels. *Composite Structures*, 89, 159–166.

Sahin, O. S., Akdemir, A., Avci, A., & Gemi, L. (2008). Fatigue crack growth behavior of filament wound composite pipes in corrosive environment. *Journal of Reinforced Plastics and Composites*, in press.

Samanci, A., Avci, A., Tarakcioglu, N., & Sahin, O. S. (2008). Fatigue crack growth of filament wound GRP pipes with a surface crack under cyclic internal pressure. *Journal of Material Science,* 48, 5569–5573.

Shyr, T. W., Pan, Y. H. (2003). Impact resistance and damage characteristics of composite laminates. *Composite Structures*, 62, 193-203.

Silva, R. V. (2008). Curaua/glass hybrid composite: the effect of water aging on the mechanical properties. *Journal of Reinforced Plastics and Composites*, in press.

Sun, X. K., Du, S. Y., & Wang, G. D. (1999). Bursting problem of filament wound composite pressure vessels. *International Journal of Pressure Vessels and Piping,* 76, 55–59.

Tarakcioglu, N., Akdemir, A., & Avci, A. (2001). Strength of filament wound GRP pipes with surface crack. *Composites*, Part B, 32, 131-138.

Tarakcioglu, N., Gemi, L., & Yapici, A. (2005). Fatigue failure behavior of glass/epoxy ±55 filament wound pipes under internal pressure. *Composites Science and Technology*, 65 703–708.

Tarakcioglu, N., Samanci, A., Arikan, H., & Akdemir, A. (2007). The fatigue behavior of $[\pm 55^\circ]_3$ filament wound GRP pipes with a surface crack under internal pressure. *Composite Structures*, 8 (2), 207–211.

Tarfaoui, M., Gning, P. B., & Collombet, F. (2007). Residual strength of damaged glass/epoxy tubular structures. *Journal of Composite Materials*, 41, 2165-2183.

Tarfaoui, M., Gning, P. B., Davies, P., & Collombet, F. (2007). Scale and size effects on dynamic response and damage of glass/epoxy tubular structures. *Journal of Composite Materials*, 41, 547-559.

Tarfaoui, M., Gning, P. B., & Hamitouche L. (2008). Dynamic response and damage modeling of glass epoxy tubular structures: Numerical investigation. *Composites*, Part A 39, 1–12.

Xu, P., Zheng, J. Y., & Liu, P. F. (2009). Finite element analysis of burst pressure of composite hydrogen storage vessels. *Materials and Design*, 30, 2295–2301.

Velosa, J. C., Nunes, J. P., Antunes, P. J., Silva, J. F., & Marques, A. T. (2009). Development of a new generation of filament wound composite pressure cylinders. *Composites Science and Technology*, 69, 1348–1353.

Wakayama, S., Kobayashi, S., İmai, T., & Matsumoto, T. (2002). Evaluation of burst strength of FW-FRP composite pipes after impact using pitchbased low-modulus carbon fiber. *Composites*, Part A, 37, 2002-2010.

Yaylagan, E. (2010). *Failure pressure of composite cylinders with a plastic liner. Master of Science thesis*. Izmir: Faculty of School Natural and Applied Sciences of Dokuz Eylul University.

Zheng, J. Y., & Liu P. F. (2008). Elasto-plastic stress analysis and burst strength evaluationof Al-carbon fiber/epoxy composite cylindrical laminates. *Computational Materials Science*, 42, 453–461.

Zou, Z., Reid, S. R., Li, S., & Soden P. D. (2002). Application of a delamination model to laminated composite structures. *Composite Structures,* 56, 375–389.